

İZMİR KATİP ÇELEBİ UNIVERSITY
GRADUATE SCHOOL OF NATURAL AND APPLIED SCIENCES

**DESIGN AND DEVELOPMENT OF THE COMPOSITE HYDROGEN
STORAGE TANKS BY USING STOCHASTIC OPTIMIZATION METHODS**



M.Sc. THESIS

Ozan AYAKDAŞ

Department of Mechanical Engineering

JUNE 2018

İZMİR KATİP ÇELEBİ UNIVERSITY
GRADUATE SCHOOL OF NATURAL AND APPLIED SCIENCES

**DESIGN AND DEVELOPMENT OF THE COMPOSITE HYDROGEN
STORAGE TANKS BY USING STOCHASTIC OPTIMIZATION METHODS**



M.Sc. THESIS

Ozan AYAKDAŞ
(Y140105010)

Department of Mechanical Engineering

Thesis Advisor: Assist. Prof. Dr. Levent AYDIN

JUNE 2018

İZMİR KATİP ÇELEBİ ÜNİVERSİTESİ
FEN BİLİMLERİ ENSTİTÜSÜ

YÜKSEK BASINÇLI KOMPOZİT HİDROJEN DEPOLAMA TANKLARININ
STOKASTİK OPTİMİZASYON YÖNTEMLERİ KULLANILARAK
TASARLANMASI VE GELİŞTİRİLMESİ

YÜKSEK LİSANS

Ozan AYAKDAŞ
(Y140105010)

Makine Mühendisliği Ana Bilim Dalı

Tez Danışmanı: Dr. Öğr. Üyesi Levent AYDIN

HAZİRAN 2018

Ozan AYAKDAŞ a M.Sc. student of **İKÇU Graduate School Of Natural And Applied Sciences**, successfully defended the thesis entitled “**DESIGN AND DEVELOPMENT OF THE COMPOSITE HYDROGEN STORAGE TANKS BY USING STOCHASTIC OPTIMIZATION METHODS**” which he prepared after fulfilling the requirements specified in the associated legislations, before the jury whose signatures are below.

Thesis Advisor :

Assist. Prof. Dr. Levent AYDIN
İzmir Katip Çelebi University

Jury Members :

Assist. Prof. Dr. Sercan ACARER
İzmir Katip Çelebi University

Assist. Prof. Dr. Sinan KANDEMİR
İzmir Institute of Technology

Date of Submission : 01.06.2018

Date of Defense : 12.06.2018





To my family,



FOREWORD

I would like to express my sincere gratitude to my supervisor Assist. Prof. Dr. Levent Aydın and my Tubitak project group TÜBİTAK project 215M182. for his advises, guidance, support, encouragement, and inspiration through the thesis. His patience and kindness are greatly appreciated. I also grateful my project administrator Assoc. Prof. H. Seçil Artem for her guidance, support and encouragement. I am also grateful for grant 215M182 project provided by The Scientific and Technologies Research Council of Turkey (TUBİTAK). My thesis study which is a just part of this project was made possible thanks to this grant. I would also thank to Melih Savran, Harun Sayı, Mehmet Akçair and Aynur Ayvalık for their support, encouragement and contributions. I offer sincere thanks to Seda Özhan for her love, support and encouragement. Lastly, the endless gratitude my family for supporting and encouraging me during my undergraduate and postgraduate studies.

JUNE 2018

Ozan AYAKDAŞ



TABLE OF CONTENTS

	<u>Page</u>
FOREWORD	ix
TABLE OF CONTENTS	xi
LIST OF TABLES	xv
LIST OF FIGURES	xvii
ABSTRACT	xix
ÖZET	xxi
1. INTRODUCTION	1
1.1 Literature Survey.....	1
1.2 Objectives.....	4
2. HYDROGEN STORAGE TECHNOLOGIES	5
2.1 Hydrogen Storage Systems	5
2.1.1 Physical Storage	7
2.1.1 Chemical Storage	8
2.2 Types of Hydrogen Storage Tanks	8
2.3 Industrial Applications of Hydrogen Storage Tanks.....	9
2.3.1 Automotive Applications	9
2.3.2 Marine Applications	10
2.3.3 Aerospace Applications	11
2.4 Manufacturing Types of Hydrogen Storage Tanks.....	12
2.4.1 Filament Winding	12
2.4.2 Tow Preg Winding	13
3. COMPOSITE MATERIALS	15
3.1 Introduction	15
3.2 Classification of Composites.....	18
C4. MECHANICS OF COMPOSITE MATERIALS	23
4.1 Classical Laminated Plate Theory.....	24
4.2 Stress Analysis of the Type III and Type V Composite Tanks.....	28
4.3 Failure Analysis in Composite Pressure Vessels	30
4.3.1 Isotropic cases	31
4.3.2 An-isotropic cases	31
5. OPTIMIZATION	33
5.1 Single Objective Optimization.....	34
5.2 Multi Objective Optimization	34
5.3 Stochastic Optimization Algorithms	35
5.3.1 Differential Evolution Algorithm.....	35
5.3.2 Nelder Mead Algorithms	36
5.3.3 Simulated Annealing Algorithm	38
6. VERIFICATION PROBLEMS	41
6.1 Problem V1	44
6.2 Problem V2	47
6.3 Problem V3	51
6.4 Problem V4	52
6.6 Problem V5	54
7. OPTIMIZATION PROBLEMS	57

7.1 Definitions for Problem 1, 2 and 3	59
7.2 Design Results of the Problem 1, 2 and 3	62
7.3 Problem 4	64
7.4 Problem 5	66
7.5 Problem 6	67
8. CONCLUSION	71
REFERENCES	75
CURRICULUM VITAE	81







LIST OF TABLES

	<u>Page</u>
Table 2.1 : Comparison of main hydrogen storage media[27-28]	6
Table 3.1 : Specific Modulus and Specific Strength Values of Typical Fibers, Composites and Bulk Metals[43].....	17
Table 3.2 : Differences between thermosets and thermoplastics [43].....	20
Table 3.3 : Comparison of Conventional Matrix Materials[45].....	21
Table 3.4 : Advantages and disadvantages of reinforcing fibers[45].....	22
Table 5.1 : Three optimization methods options.....	38
Table 6.1 : Table of the Problem Verifications.....	43
Table 6.2 : Mechanical properties of Graphite /Epoxy composite materials[46]	44
Table 6.3 : Strength parameters of Graphite /Epoxy composite materials[46].....	44
Table 6.4 : Comparison Results of present thesis and the study by Pelletier and Vel[46] for burst pressure calculations	45
Table 6.5 : Comparison Results of present thesis and the study by Pelletier and Vel[46] for hoop rigidity and areal mass density.....	46
Table 6.6 : Design constraints used in problem V2	48
Table 6.7 : Comparison of the results of the hoop rigidity by using DE, SA and NM	48
Table 6.8 : Comparison of the results of the stacking sequences design by using DE, SA and NM	49
Table 6.9 : Comparison of the results of the areal mass density by using DE, SA and NM	50
Table 6.10 : Comparison of the results of the burst pressure by using DE, SA and NM.	51
Table 6.11 : Mechanical properties of T6061 Al and T700 Carbon/Epoxy composite materials[61]	51
Table 6.12 : Strength parameters of T700 Carbon/Epoxy composite materials[61].	52
Table 6.13 : Comparison of the burst pressure calculations based on numerical and analytical approaches with the experimental one	52
Table 6.14 : Mechanical properties of T6061 Al and T700 Carbon/Epoxy composite materials[24]	53
Table 6.15 : Strength parameters of T700 Carbon/Epoxy composite materials[24].	53
Table 6.16 : Results of the Tsai-Wu and Maximum Stress failure indexes.....	53
Table 6.17 : Mechanical properties of T6061 Al and T700 Carbon/Epoxy composite materials[62]	54
Table 6.18 : Strength parameters of T700 Carbon/Epoxy composite materials[62].	54
Table 6.19 : Geometrical Dimensions of the Type-III Pressure Vessel[62]	54
Table 6.20 : Comparison of the burst pressure for Problem V5	55
Table 7.1 : Optimization Problems	58
Table 7.2 : Mechanical properties of T6061 Al and T700 Carbon/Epoxy composite materials.	59
Table 7.3 : Strength parameters of T700 Carbon/Epoxy composite materials[62]...	59
Table 7.4 : Results of the Problems.....	63
Table 7.5 : Mechanical Properties of the materials.....	64

Table 7.6 : Optimization results of the Problems 4 for different Carbon/ Epoxy composites	65
Table 7.7 : Results of the Problems 5.....	67
Table 7.8 : Mechanical properties of T6061 Al and T700 Carbon/Epoxy composite materials[24].....	68
Table 7.9 : Strength parameters of T700 Carbon/Epoxy composite materials[24]...	68
Table 7.10 : Optimum results of the stacking sequences design for problem 6.....	69



LIST OF FIGURES

	<u>Page</u>
Figure 2.1 : Overview of hydrogen storage systems and materials [29]	7
Figure 2.2 : Tank Types and manufacturing, burst test of Type III, IV or V [33].....	9
Figure 2.3 : Toyota mirai fuel cell system [36]	10
Figure 2.4 : Zemships project – fcs alsterwasser [37].....	10
Figure 2.5 : Fuel cell boat amsterdam. [37]..	11
Figure 2.6 : Hydrogen tanks on plane model [38].	11
Figure 2.7 : Toyota mirai fuel cell system [36]	12
Figure 3.1 : Specific strength as a function of time of use of materials [43].....	16
Figure 3.2 : Composite types according to reinforcement shape [43].	18
Figure 4.1 : A thin fiber-reinforced laminated composite	24
Figure 4.2 : Coordinate locations of plies in a laminate [43].....	25
Figure 5.1 : Flowchart of the DE algorithm.	36
Figure 5.2 : Flowchart of the NM algorithm. [59].....	37
Figure 5.3 : Flowchart of the SA algorithm. [60]	39
Figure 6.1 : Cylindrical Part of the Type III Pressure Vessel	41
Figure 6.2 : Cylindrical Part of the Type V Pressure Vessel	42
Figure 7.1 : Configuration of the Type III and Type V Pressure Vessel	57



DESIGN AND DEVELOPMENT OF THE HYDROGEN STORAGE TANKS BY USING STOCHASTIC OPTIMIZATION METHODS

ABSTRACT

In this thesis, there are five main objectives: (i) To calculate stress and strain components based on CLPT for only composite (Type IV and Type V) and aluminum-composite (Type III) pressure vessels (ii) To determine the burst pressure based on Classical Laminated Plate Theory and first ply failure theories for the cylindrical part of the Type III and Type V composite pressure vessels (iii) to compare the analytically calculated burst pressure values with the experimental and Finite Element Methods results in the literature (iv) to propose optimum stacking sequences designs for Type III and Type V tanks having 70 MPa working pressure with 2, 2.25 and 2.5 safety factors against burst by using interactive, non-interactive and partial interactive first ply failure theories as for the objective functions and constraint, simultaneously (v) to compare the computational performance of the optimization algorithms; Differential Evolution (DE), Simulated Annealing (SA) and Nelder Mead (NM) for composite pressure vessel design problems. In the thesis, the Type III hydrogen storage tanks are assumed as consist of an inner metallic liner and laminated Carbon/Epoxy or Graphite/Epoxy composite layers. Type V tanks are also considered as including only composite layers. In order to predict the failure indexes and burst pressure of the tank, Hashin-Rotem, Maximum Stress and Tsai-Wu first ply failure criteria have been employed. The optimization algorithms DE, SA and NM have given the applicable results for composite hydrogen storage tanks designs problems. Due to be symmetric balanced and integer features of the composites, manufacturable stacking sequences design have been achieved.



YÜKSEK BASINÇLI KOMPOZİT HİDROJEN DEPOLAMA TANKLARININ STOKASTİK OPTİMİZASYON YÖNTEMLERİ KULLANILARAK TASARLANMASI VE GELİŞTİRİLMESİ

ÖZET

Bu tezde beş ana amaç vardır: (i) Sadece kompozit (Tip IV ve Tip V) ve alüminyum-kompozit (Tip III) basınçlı kaplar için Klasik Laminasyon Teorisini kullanarak gerilme ve şekil değişim bileşenlerini hesaplamak (ii) Tip III ve Tip V kompozit basınçlı kapların patlama basıncını Klasik Laminasyon Teorisi ve birinci tabaka kırılma teorilerini kullanarak hesaplamak (iii) kompozit tankların silindirik kısımları için birinci tabaka kırılma teorilerine dayalı olarak hesaplanan patlama basıncı değerlerinin, literatürden alınan deneysel ve sonlu elemanlar yöntemleri sonuçları ile karşılaştırılmak (iv) interaktif, interaktif olmayan ve kısmi interaktif birinci tabaka kırılma teorilerini, amaç fonksiyonunda ve kısıtlarda eş zamanlı olarak kullanarak, patlamaya karşı 2, 2.25 ve 2.5 güvenlik faktörleri ile 70 MPa çalışma basıncına sahip Tip III ve Tip V tankları için optimum istifleme dizileri tasarımlarını önermek (v) Kompozit basınçlı kap tasarım problemleri için Diferansiyel Evrim (DE), Simüle Tavlama (SA) ve Nelder Mead (NM) optimizasyon algoritmalarının hesaplama performansını karşılaştırmak. Bu tezde, Tip III hidrojen depolama tanklarının, bir iç metalik astar ve lamine Karbon / Epoksi veya Grafit / Epoksi kompozit tabakalardan oluştuğu varsayılmaktadır. Tip V tankların sadece kompozit tabakaları içerdiği düşünülmektedir. Hidrojen depolama tanklarının patlama basıncını tahmin etmek için Hashin-Rotem, Maksimum Stres ve Tsai-Wu birinci tabaka kırılma kriterleri kullanılmıştır. DE, SA ve NM optimizasyon algoritmaları, kompozit hidrojen depolama tankları problemleri için uygulanabilir sonuçlar vermiştir. Kompozitlerin simetrik ve tamsayı özellikleri nedeniyle, imal edilebilir tabaka sarım açıları tasarımı gerçekleştirilmiştir.



1. INTRODUCTION

1.1 Literature Survey

Increasing energy demand, climate change and environmental pollution direct humanity to create clean and renewable energy opportunities. As an alternative resource hydrogen has been arising due to its highest energy density (120 MJ/ kg) in terms of mass among all other fuels. In this point, two critical problems can be overcome with hydrogen. These are (i) clean transportation and (ii) consuming without polluting the environment. From storage point of view, hydrogen can be stored with different types such as; onboard the automobiles as highly compressed gas, cryo-compressed liquid, or in advanced storage materials. Moreover, after the commercialization efforts, composite pressure vessels attracted more interest due to their low weight and, they are able to store hydrogen as highly compressed gas. Additionally, these hydrogen storage composite pressure vessels can be used in many industrial areas such as power plant, aerospace, chemical and automotive industry [1]. Especially, automotive and aerospace industrial applications need lightweight structures such as composite pressure vessels. Therefore, many researchers have investigated the design and optimization of lightweight composite pressure vessels. Statistical studies in the literature show that the strength of composite hydrogen storage tanks is designed and optimized by changing the laminate stacking sequence. Additionally, the correlation between the fiber volume and vessel strength is important. The strengths of composite pressure vessels also depend on fibre volume in the hoop layers [1].

There are several studies conducted on composite hydrogen storage vessels. All of these studies admit the difficulties of decreasing high cost and weight and increasing burst strength and load capacities [2-11]. In a previous study, an analytical model has been established and stacking sequences of composite cylinders has been optimized by using genetic algorithm[12]. The results have been compared with those of experiments and numerical analysis, and good agreement has been found. However,

for more complicated filament wound composite structures, optimal designs have not been reported in the literature yet. The researchers studied on the design procedure of composite pressure vessel and the Classical Laminated Plate Theory and Tsai-Wu failure criterion have been used to obtain the single optimum winding angle [13]. The optimum fiber orientation angles have been found to be 52.1 and 54.1 degrees depending on different material types. As a stochastic optimization method, Genetic Algorithms (GA) has been utilized in order to optimize cylindrical part of the composite pressure vessel by making the three-dimensional stress-strain calculation [14]. A composite internal pressurized pipe optimization problem for single angle has been solved for different materials such as E-glass, Carbon and Kevlar fiber reinforced composites. Finally, optimum fiber orientation angles have been found as 53.2, 54.3 and 54.9 degrees, respectively [15]. The optimal design algorithm for Type III filament wound vessels has been developed by Kim et al. [16]. The objective functions have been selected as weight and failure. The GA has been also utilized to solve optimization problems, and they proposed some stacking sequences designs. However, in this study, a single orientation angle has been chosen from the various angle constraints. In order to reduce the weight of the pressure vessel, Finite Element Method (FEM) and GA have been collaborated in optimization procedure by Tomasetti et al. [17]. To determine the optimum weight under the Tsai Wu failure constraint, Type III hydrogen storage tanks have been designed using the artificial immune system (AIS) method [18]. Single winding angle has been optimized depending on the opening radius of the vessel in this study. Some designs have been proposed to have burst pressure of 150 MPa. An adaptive genetic algorithm has been used to optimize the composite pressure vessel and compared with a simple genetic algorithm and a Monte Carlo optimization method [19]. After this optimization procedure, some pressure vessel designs having a burst pressure 164.5 MPa have been obtained for the different radii. The comparison of the different optimization methods for Type III tanks have been carried out by using Classical Laminated Plate Theory (CLPT) and FEM with Reddy's progressive damage law [20]. This study shows that optimization strategy is important in the view of selection which first ply failure and final failure. For Type IV pressure vessel which can store about 5.8 kg hydrogen at 70 MPa, Roh et al.[17] have focused on the design-optimization problems. In the study, the plastic liner and opening boss have not been considered in the analysis. Therefore, Type IV analysis has been carried out similar to Type V hydrogen storage tanks. Recently, another study

[22] focused on the weight minimization problem of Type IV hydrogen storage tank by using genetic algorithms and simulated annealing [22]. CLPT and Tsai-Wu failure criterion have been utilized to design pressure vessels having a burst strength against to 70 MPa working pressure with a safety factor of 2.25. It was shown that the proposed methodology produced more efficient designs by reducing the weight up to 9.8% and 11.2 %.

In the optimization study of the Type III pressure vessel with metallic liner, Adaptive Response Surface Method [ARSM] were applied to solve the highly nonlinear functions related to FEM [23]. As a result of the study, computation time has been importantly decreased and optimum design has been found for Type III CNG vessels. In the study [24] Type III pressure vessel optimum design results have been analyzed by using FEM. The total composite thickness is taken as objective function and it is found that the weight of the vessels decreased between 5.7% and 7.1.

Traditional and non-traditional methods have been used in various composite optimization problems. Due to the complexity of the composite pressure vessel design problems considerations, the traditional methods have not been chosen to optimize. In these cases, the algorithms like Particle Swarm Algorithms (PS), Genetic Algorithms (GA), Generalized Pattern Search Algorithm (GPSA), and Simulated Annealing (SA) have been found to use appropriately. Derivative calculations or approximations are impossible to obtain or often costly in the design and optimization of composites so stochastic search methods may be more efficient for the optimization process [25]. Fiber orientation angles and thickness are generally design variables in fibre-reinforced composite hydrogen storage tanks design and optimization studies [26].

After covering the literature survey, it is seen that there are some deficiencies for design and optimization procedure of composite pressure vessels. For example, there is no definite information on the optimization approach which it could be called the best. Among the stochastic optimization methods, some algorithms may be better for some problems, while others may give worse results. Various failure theories such as Tsai-Wu, Maximum Stress, Hoffman, Tsai-Hill and Hashin have been used for composite pressure vessel designs. However, in general, Tsai-Wu failure criterion is widely used compared to other theories.

In this thesis, the unsolved design and optimization problems have been tried to overcome for composite hydrogen storage tanks.

1.2 Objectives

The main objectives of this thesis can be listed as follows:

- 1) To calculate stress and strain components based on CLPT for only composite (Type V and Type IV) and aluminium-composite (Type III) pressure vessels
- 2) To calculate failure indexes by using first ply failure theories and Von Mises yield criterion for only composite (Type V and Type IV) and aluminium-composite (Type III) pressure vessels
- 3) To determine the burst pressure based on Classical Laminated Plate Theory and first ply failure theories for cylindrical part of the Type III and Type V composite pressure vessels
- 4) To compare the analytically calculated burst pressure values with the experimental, analytical and FEM results in the literature
- 5) To design optimum stacking sequences having 70 MPa working pressure with 2, 2.25 and 2.5 safety factors against burst for Type III aluminium-composite pressure vessel
- 6) To optimize composite pressure vessel by using interactive, non-interactive and partial interactive first ply failure theories as the objective functions and constraint, simultaneously
- 7) To propose different optimum stacking sequences designs for Type V and Type III hydrogen storage vessels for different materials
- 8) To compare the computational performance of the optimization algorithms; DE, SA and NM for composite pressure vessel design problems
- 9) To compare the optimization results obtained by DE, SA and NM with one of the popular algorithm (Genetic Algorithm) used in the literature
- 10) To compare optimum stacking sequences design of the Type III and Type V composite pressure vessels for different Carbon/ Epoxy materials by DE methods

2. HYDROGEN STORAGE TECHNOLOGIES

Today, largest energy production relies on fossil fuels. However, it is expected that fossil fuels will not be main energy source in the future due to their disadvantages such as nonrenewable feature and huge emissions of greenhouse gases. Regarding these facts, the researchers focus on to produce alternative energy resources and hydrogen is studied as a candidate energy source for fossil fuels. The main advantage of H₂ is that it has highest energy density of all common fuels by weight. It can also be stored onboard the automobiles as high compressed gas, cryo-compressed liquid, or in advanced storage materials. In vehicles, from a commercialization point of view, high compressed gas cylinders and, cryogenic tanks the storage systems seem to be advantages. Therefore, many researches are studied on H₂ storage methods involving the features sustainable, safe, reliable and low cost. The hydrogen storage systems can be used in many industrial applications, such as, power plant, aerospace, chemical and automotive industry

This Chapter will provide an overview of the state of the art in the engineering of hydrogen storage technologies over a wide range of industries.

2.1 Hydrogen Storage Systems

Hydrogen storage systems can be categorized as: (i) physical storage (compressed gas, cryogenic); and (ii) storage in solid materials (physisorption, chemical storage). Practically, gravimetric and volumetric energy densities are used to investigate the appropriateness of storage medium for the applications [27]. Available hydrogen storage technologies, density-pressure-temperature and cost values are compiled in Table 2.1 [28].

Table 2.1 : Comparison of main hydrogen storage media [27-28].

Storage Technologies	Volumetric Density (kg H ₂ / m ³)	Gravimetric density (reversible) (wt.%)	Operating pressure (bar)	Operating temperature (K)	Cost* (\$/kg H ₂)
Compressed gas (H ₂)	17-33	3-4.8 (system)	350-700	Ambient	400-700*
Cryogenic (H ₂)	35-40	6.5-14 (system)	1	20	200-270*
Cryo-compressed (H ₂)	30-42	4.7-5.5 (system)	350	20	400
High pressure-solid	40	2 (system)	80	243-298	
Sorbents (H ₂)	20-30	5-7 (material)	80	77	
Metal hydrides (H)	<150	2-6.7 (material)	1-30	Ambient-553	>500
Complex hydrides (H)	<120	4.5-6.7 (material)	1-50	423-573	300-450**
Chemical hydrides (H)	30	3-5 (system)	1	353-473	160-270***

* Off-board regeneration required. ** Cost estimates based on 500 000 units production.
*** Regeneration and processing costs not included.

Materials used in physical storage applications are generally referred to improve the structure of the vessels. A detail classification of hydrogen storage systems and the materials with some selected hydrides are given in Fig. 1

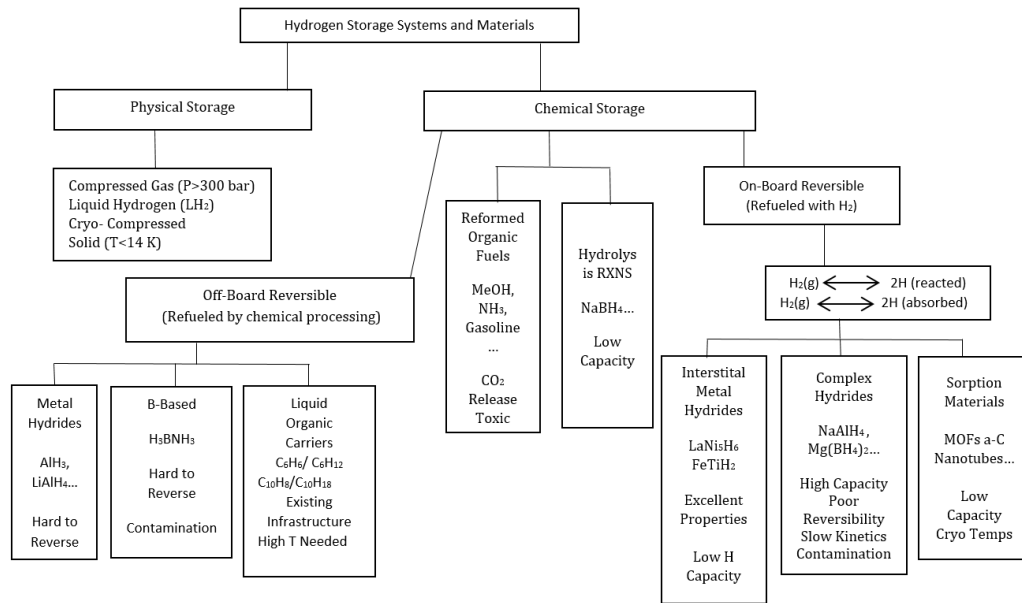


Figure 2.1 : Overview of hydrogen storage systems and materials [29].

2.1.1 Physical storage

Physical storage are generally categorized as (i) compressed gaseous hydrogen, (ii) liquid hydrogen and (iii) Cryoadsorption on high-surface-area materials. If the work space is relatively small, the use of 35–70 MPa compressed gaseous hydrogen is appropriate. So as to reach the automobiles with a range of about 500 km, it is required that 5–6 kg of hydrogen on board in the car. Three to five minutes is enough to refill compressed gaseous hydrogen tanks [30]. When working with pressure values greater than 70 MPa, special vessel designs are required [30]. A detailed analysis of design and optimization of hydrogen storage tanks are described in section 6.

Another important physical storage system is liquid hydrogen. It uses the features high mass density of hydrogen at -253 °C and 0.1 MPa. The usable volumetric storage density is slightly higher compared to compressed gaseous hydrogen systems.

In addition to this, almost all the companies in automotive industry think that the use of liquid hydrogen tanks are not very advantages [29].

Third physical storage system “Cryoadsorption”(on high-surface-area materials, 0.2–0.5 MPa,-193 °C) generally uses Zeolites, Carbon and Metal–Organic Frameworks adsorbents

“Currently, the physical storage technologies, and in particular CGH₂ and LH₂ are most mature; most prototypes of fuel-cell-powered cars use one of these storage systems. 70 MPa CGH₂ is considered to be the state-of-the art technology” [29].

2.1.2 Chemical storage

The main chemical compounds and materials utilized for hydrogen storage are (i) metal hydrides; (ii) complex hydrides; (iii) borohydrides; (iv) alanes and alanates; and (v) nitrides, imides and amides. A chemical hydrogen storage tank is basically a reservoir containing a hydrogenated compound. In industrial applications, individual hydride reactors adjust the storage capacity of miscellaneous stationary end-uses [29].

2.2 Types of Hydrogen Storage Tanks

Five types (Type I-V) of pressure vessels are used for hydrogen storage. The selection of the type is based on the application area and technical performance, cost and weight. In Type I tank (all-metal cylinders), the pressure level is 150 to 300 bar [31]. Type I pressure vessels are the cheapest and therefore widely used in industry. Type II pressure vessels have only hoop-wrapped composite on a metallic liner and these type tanks are preferred for stationary applications. Type III tanks are also been wound fully composite on metallic liners. There are generally three type wound style; helical, hoop and geodesic form. Type IV tanks are the usage of plastic liners instead of metallic liners on Type III tanks. Type V tank is also having no liner and it is composed of fully wrapped composites windings. Advantages of Type IV and V pressure vessels are that it has low weight by comparison Type III tanks. However, in type IV and V tanks, sealing the hydrogen gas and handling of the stress is more important issues than Type III tanks. Type III, IV and V pressure vessels are particularly preferred in applications where weight saving is important. However, the disadvantage of these vessels is high cost [32].

The material of the port is metal and it is integrated into boss. The tanks are generally cylinders, but composite hydrogen storage tanks can also be polymorph or toroid (Figure 2.2).

The tensile strength (σ_v) of the storage tank material is an essential parameter. Therefore, carbon fiber is used to obtain high strength values for 350 and 700 bar

hydrogen storage tanks. This also provides hydrogen system capacities of 5.9% and - 4.7% by weight, respectively [34].

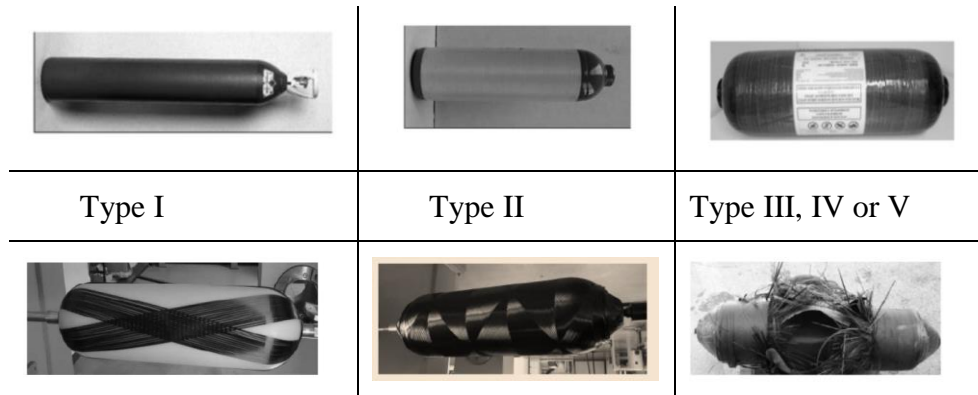


Figure 2.2 : Tank Types and manufacturing, burst test of Type III, IV or V [33].

2.3 Industrial Applications of Hydrogen Storage Tanks

Hydrogen storage is one of the most important step toward the hydrogen economy. However, they have to be stored before the usage because of its uneven distribution. In this section, the application fields (automotive, marine, aerospace) of the hydrogen storage tanks have been summarized.

2.3.1 Automotive applications

In automotive applications, hydrogen requirements stored on-board for 400 km transport range is 4 kg. The main design targets are (i) 100 kg for total system weight (ii) 150 L for total volume corresponding to a gravimetric density of 4 wt.% (1.33 kWh/kg) and a volumetric density of 2.7×10^{-2} kg/L of hydrogen. Refilling process yields approximately 5 min for a 5 kg hydrogen load [35]. As a recent on board application of hydrogen fuel cell system involving the location and working process elements for Toyota mirai are shown (Figure 2.3).

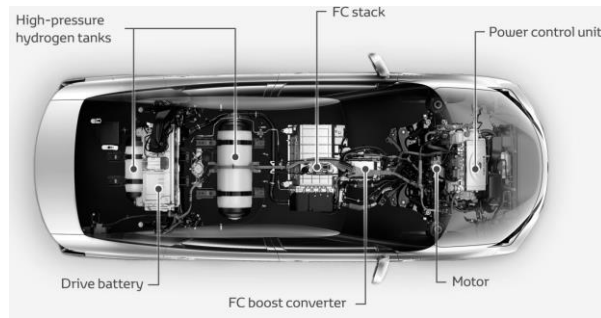


Figure 2.3 : Toyota mirai fuel cell system [36].

2.3.2 Marine applications

Zemships project (2007-2010)

The Zemships project founded by the EU-Life program, is the first project in the world utilizing hydrogen fuel cells system on a commercial passenger ship. Two fuel cell systems are combined with a peak output of 48 kW each with a 560-V lead gel battery pack (see Figure 2.4). Practically, a prototype (FCS ALSTERWASSER) has been designed and produced. The length is 25.50 m, while width is 5.25 m and the passenger transport capacity is 100. Project partners are reported in [37] as Hamburg University of Applied Science, ATG Alster Touristik, Germanischer Lloyd, Hochbahn, hySOLUTIONS, Linde Group, Proton Motor, UJV Nuclear Research Institute. It should be noted that the ship started its operation in August, 2008.

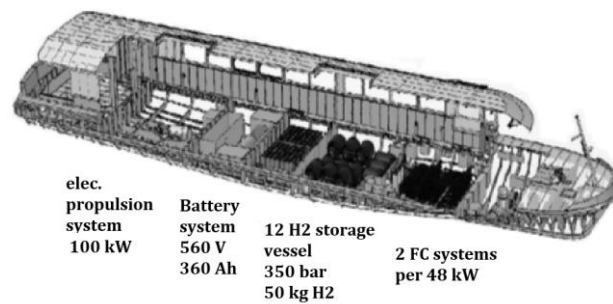


Figure 2.4 : Zemships project – fcs alsterwasser [37].

Fuel cell boat BV project

The second marine application project example is Fuel Cell Boat BV (Figure 2.5). The main objective of the design is to realise an inland passenger vessel with a hydrogen fuel cell system. The system also involves the infrastructure for the refuelling of the tank. The main features of the Fuel Cell Boat BV are (i) length is 22 m, (ii) width is 4.25 m, (iii) power of hydrogen fuel cell system is 60-70 kW, (iv) the passenger limit is 100. The certification is done by Germanischer Lloyd. The ship have been in operation since December of 2009 [37].

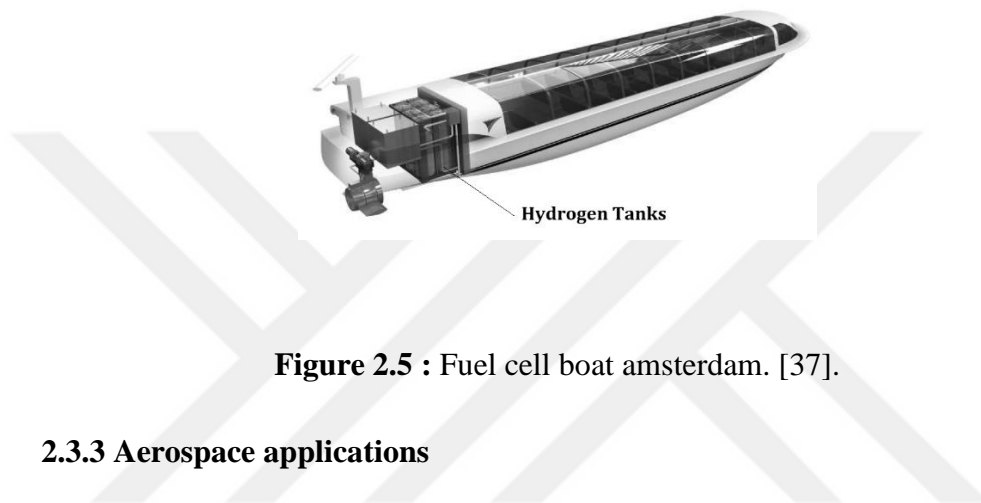


Figure 2.5 : Fuel cell boat amsterdam. [37].

2.3.3 Aerospace applications

AVIZOR project

The initial configuration of the project envisages the use of compressed hydrogen and PEM fuel cells (Figure 2.6). The AVIZOR system consists of fuel cell with batteries, engine with controller and fuel storage. The general features of the system are: (i) the volume of the one storage tank is 25 L, (ii) the weight of the tank is 15 kg, (iii) working and burst pressures of hydrogen tank are 350 and 750 bars, respectively (iv) weight of the stored hydrogen is 1.6 kg, (v) The oxidant is high pressure gaseous oxygen and the storage system is a tank to 200 bar [38].

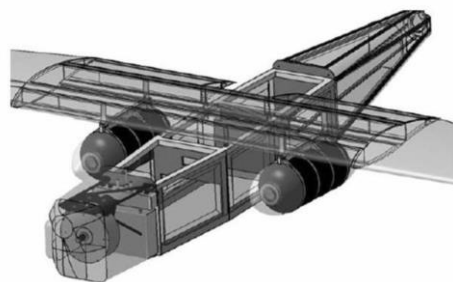


Figure 2.6 : Hydrogen tanks on plane model [38].

2.4. Manufacturing Types of Hydrogen Storage Tanks

The main manufacturing processes of high pressure hydrogen storage tanks are filament winding and tow preg winding methods. In order to obtain good designs for the tanks, it is necessary to consider balance between multiple technical requirements involving cost and government specifications [39]. Therefore, the selection of manufacturing methods depend on this balance.

2.4.1. Filament winding

In filament winding process, firstly, fibre tows are passed through a resin bath, secondly, resin-impregnated rovings band or monofilaments is wrapped around a rotating mandrel in order to produce axisymmetric hollow parts. The schematic representation of filament winding process is also given in Figure 7. The essential parameters in a filament-winding process are (i) fiber tension, (ii) fiber wet-out, and (iii) resin content [40]. In general use of it, four axes winding are preferred since more complicated geometric productions are possible. With the aid of advanced machine control ability, recent filament winding process machines are also provide an opportunity for manufacturing non-cylindrical and/or non-symmetric objects.

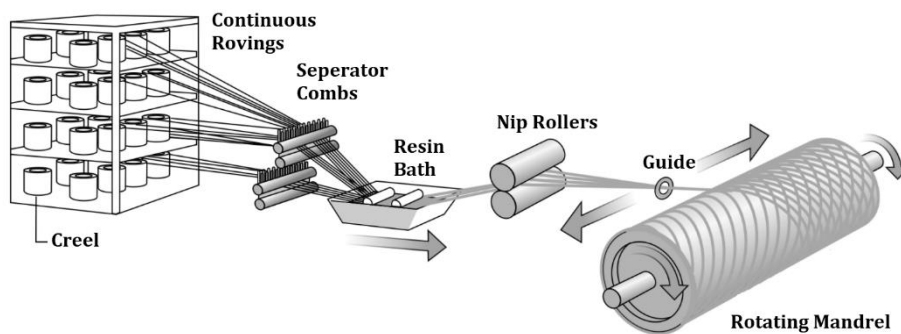


Figure 2.7 : Filament winding process [42].

2.4.2 Tow preg winding

The tow-preg filament winding production process can be applied as an alternative to wet-filament winding and also has some advantages. These advantages are (i) setup and cleanup time is better, (ii) higher laminate quality with lower weight, (iii) production pollution is lower (iv) winding speed does not affected by the fiber wetout requirements. (v) for large scale of carbon-Epoxy pressure vessels, cost is applicable,(vi) curing process is relatively easy [41].





3. COMPOSITE MATERIALS

3.1 Introduction

Composite materials consist of two or more constituent called reinforcement phase and matrix. These components are not soluble in each other at the macroscopic level. Particles, fibers or sheet forms are selected as geometry of reinforcement material while matrix materials are generally chosen between the natural and continuous materials. The generally used composites examples are carbon fiber reinforced epoxy and steel reinforced concrete [43].

The usage of composite materials has continued for many centuries. For example, during the building of pyramids, the bricks were used by putting chopped straw in order to increase integrity of the pyramids. Eskimos used moss to carry out strength ice homes. In Japanese, the Samurai warriors utilized multilayered metals during the forging in order to increase material properties of their swords. In the 20th century, before using fiberglass polymer composites throughout the World War II, first well known professionally usage of the composite is that civil engineers carried out to produce reinforced concrete by placing iron into the cement [44].

Fiber-reinforced composite materials have low density, high specific modulus (ratio between the young modulus and the density) and specific strength (ratio between strength and density). In addition to these natural features, these materials include some important design parameters to be able to tailored and provided advantage to against conventional isotropic materials. Tailorability is an important issue in development of the material features and it is possible by changing the effective parameters such as ply orientation and stacking sequence. Thus, in many engineering areas such as automotive, marine and aerospace, composites are utilized instead of metals.

Figure 3.1 demonstrates the usage of fibers, composites and the other traditional materials in terms of specific strength on annual basis.

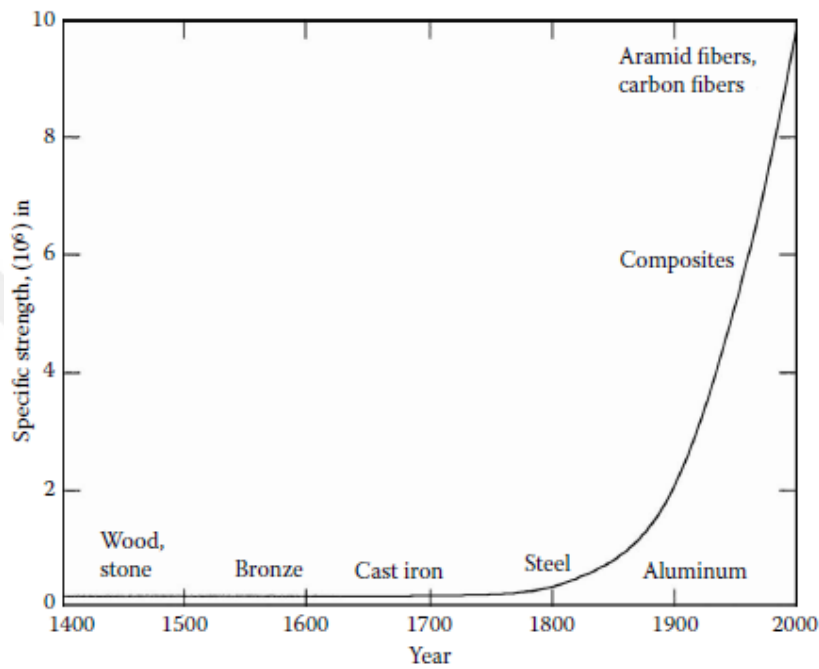


Figure 3.1 : Specific strength as a function of time of use of materials [43].

Table 3.1 shows specific strength and specific modulus features for generally used composite fibers, unidirectional composites, cross-ply and quasi-isotropic laminated composites and monolithic metals [43].

Table 3.1 : Specific Modulus and Specific Strength Values of Typical Fibers, Composites and Bulk Metals [43].

Materials Units	Specific Gravity	Young's Modulus (GPa)	Ultimate Strength (MPa)	Specific Modulus (GPa-m ³ /kg)	Specific Strength (MPa-m ³ /kg)
System of Units: SI					
Graphite fiber	1.8	230	2067	0.1278	1.148
Aramid fiber	1.4	124	1379	0.08857	0.9850
Glass fiber	2.5	85	1550	0.0340	0.6200
Unidirectional Graphite/Epoxy	1.6	181	1500	0.1131	0.9377
Unidirectional glass/Epoxy	1.8	38.60	1062	0.02144	0.5900
Cross-ply Graphite/Epoxy	1.6	95.98	373	0.06000	0.2331
Cross-ply glass/Epoxy	1.8	23.58	88.25	0.01310	0.0490
Quasi-isotropic Graphite/Epoxy	1.6	69.64	276.48	0.04353	0.1728
Quasi-isotropic glass/Epoxy	1.8	18.96	73.08	0.01053	0.0406
Steel	7.8	206.84	648.10	0.02652	0.08309
Aluminum	2.6	68.95	275.80	0.02652	0.1061

3.2 Classification of Composites

Composite materials can be divided into two main categories based on reinforcement shape and matrix type. Some of reinforcement shapes are particulates, flakes and fibers (Figure 3.2) and matrix materials are ceramics, metals and polymers.

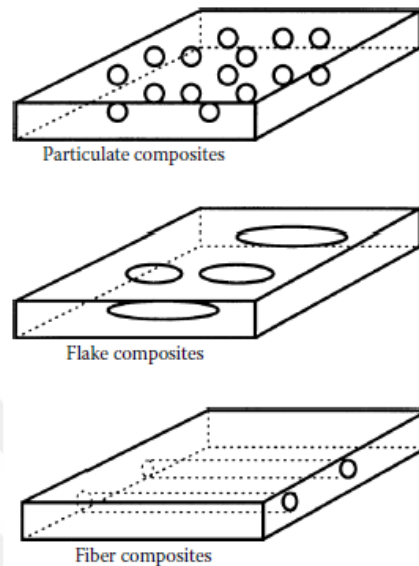


Figure 3.2 : Composite types according to reinforcement shape [43].

Including randomly scattered alloys and ceramics particles in matrix materials, particulate composites are supposed as isotropic. These composites have some advantages including advanced strength, enhanced operating temperature, and oxidation resistance. Many examples can be given on particle reinforced composites such as rubber with aluminium particles, silicon with carbide motes and concrete including gravel and sand. [43].

Another composite type is flake reinforced composites that include flat and thin reinforcements such as aluminium, glass, mica and silver in matrices. The main advantages of using flake reinforced composites is having low cost and high strength and flexural modulus. On the other hand, to change directions of the flakes are difficult. [43].

Fiber composites comprise matrices, reinforced fibers and an interface. Fibers consists of either short (discontinuous) type or long (continuous) type fiber having high aspect ratio. Carbon, Graphite, boron, kevlar and aramids are examples of fibers for composites.

Metals such as titanium, aluminum or magnesium; ceramics such as calcium–alumina silicate and resins such as epoxy, vinylester, polyester are instances of matrices. [43].

Besides being low cost, polymer matrix composites (PMCs) have high strength and simple production principles. Therefore, PMCs which comprised of reinforced by fibers having the thin diameter such as glass, graphite, boron and aramid are mostly used in the industry. Additionally, in the PMCs, polyester, urethane and epoxy are preferred as the polymer. On the other hand, PMCs have some disadvantages; (i) coefficients of thermal and moisture expansion is high (ii) in certain directions elastic properties are low and (iii) operating temperatures are low.

Carbon fibers in polymer matrix composite are used in a wide range of engineering applications. Due to having a low coefficient of thermal expansion, high fatigue strength, high-modulus and high-strength properties, carbon fibers are more often utilized in applications such as automotive, space industry, aircraft components, etc. Additionally, polymer composites based carbon fibers have some disadvantages such as high cost, low impact resistance, and high electrical conductivity. Especially, it is needed that to optimum designs should be carried out to decrease weight and usage of the materials due to be high cost for carbon fiber polymer composites. To overcome this disadvantage, glass fibers are used together with graphite in a hybrid structure. In this way, it can be provided that both suitable structural rigidity and low cost. In addition to low cost, glass fiber has advantages that high strength and chemical resistance, as well as good insulating properties. The disadvantages are low elastic modulus, poor adhesion to polymers, high specific gravity, sensitivity to abrasion (reduces tensile strength) and low fatigue strength. The main types of glass fibers are: (i) E-glass (fiberglass) is appropriate for electrical and structural applications, (ii) S-glass includes higher content of silica and keep its strength at high temperatures, (iii) C-glass (Corrosion) preferred in chemical environments, (iv) R-glass is generally utilized in structural applications, (v) D-glass (Dielectric) can be used applications entailing low dielectric constants and (vi) A-glass (Appearance) is utilized to improve surface appearance.

There are several polymers used in advanced polymer composites and classified as *thermoset* (epoxies, polyesters, phenolics, and polyamide) and *thermoplastic* (polyethylene, polystyrene, polyether–ether–ketone (PEEK) and polyphenylene sulfide (PPS)). Thermoset polymers connected strong covalent bonds are insoluble and

infusible after cure; thermoplastics include weak van der Waals bonds and thus they can be formed at high pressure and high temperatures. The diversities between thermosets and thermoplastics are denoted in Table 3.2 [43].

Table 3.2 : Differences between thermosets and thermoplastics [43].

Thermoplastics	Thermosets
Soften on heating and pressure, and thus easy to repair	Decompose on heating
High strains to failure	Low strains to failure
Indefinite shelf life	Definite shelf life
Can be reprocessed	Cannot be reprocessed
Not tacky and easy to handle	Tacky
Short cure cycles	Long cure cycles
Higher fabrication temperature and viscosities have made it difficult to process	Lower fabrication temperature
Excellent solvent resistance	Fair solvent resistance

Epoxy resins are the most commonly used thermoset in PMC, nevertheless they are more expensive than other polymer matrices. Epoxy matrices have some advantages such as high strength, low viscosity and low flow rates that permit good wetting of fibers and prevent misalignment of fibers during processing, low evaporation during cure, low shrinkage, which decrease the tendency of obtaining large shear stresses of the bond between epoxy and its reinforcement. Therefore, they are appropriate for a wide range of engineering applications.

Metal matrix composites (MMCs) comprise of metals or alloys (aluminum, magnesium, titanium, copper) reinforced with carbon (graphite), boron or ceramic fibers. The materials are commonly used to provide advantages over metals such as steel and aluminum. The main advantages of these composites can be listed as higher specific modulus and strength by low density metals such as aluminum and titanium, lower coefficients of thermal expansion, such as graphite.

Ceramic matrix composites (CMCs) include ceramic matrices (alumina calcium, silicon carbide, aluminum oxide, glass-ceramic, silicon nitride) reinforced with ceramic fibers. The main advantages of CMCs are high strength, hardness, high service

temperature limits for ceramics, chemical inertness and low density. Nevertheless, ceramic matrix composites have low fracture toughness.

Carbon-carbon composites (C/C) contain carbon fibers reinforcement in the carbon or graphite matrix. This type of composites have excellent properties of high strength at high temperature, low thermal expansion and density. Disadvantages of C/C composites are their high cost, low shear strength, and sensitivity to oxidations at high temperatures. Typical properties of conventional matrix materials are given in terms of hygro-thermo-mechanical features with their advantages and drawbacks in Tables 3.3 and 3.4.

Table 3.3 : Comparison of Conventional Matrix Materials [45].

Property	Metals	Ceramics		Polymers
		Bulk	Fibers	
Tensile strength	+	-	++	v
Stiffness	++	V	++	-
Fracture toughness	+	-	v	+
Impact strength	+	-	v	+
Fatigue endurance	+	V	+	+
Creep	v	V	++	-
Hardness	+	+	+	-
Density	-	+	+	++
Dimensional stability	+	v	+	-
Thermal stability	v	+	++	-
Hygroscopic sensitivity	++	v	+	v
Weatherability	v	v	v	+
Erosion resistance	+	+	+	-
Corrosion Resistance	-	v	v	+

++, superior; +, good; -, poor; v, variable.

Table 3.4 : Advantages and disadvantages of reinforcing fibers [45].

Fiber	Advantages	Disadvantages
E-glass, S-glass	High strength Low cost	Low stiffness Short fatigue life High temperature sensitivity
Aramid (Kevlar)	High tensile strength Low density	Low compressive strength High moisture absorption
Boron	High stiffness High compressive strength	High cost
Carbon (AS4, T300,T700,C6000)	High strength High stiffness	Moderately high cost
Graphite (GY-70, pitch)	Very high stiffness	Low strength High cost
Ceramic (silicon carbide, alumina)	High stiffness High use temperature	Low strength High cost

4. MECHANICS OF COMPOSITE MATERIALS

In engineering structures, stresses, strains and deformations are occurred as a results of mechanical and environmental effects such as moisture, temperature and radiation. The mechanics of materials consider together these effects to be able to predict the behaviour of the materials under the loading. For isotropic and homogeneous materials such as copper and stainless steel, the material properties are independent on orientation and location. For fiber reinforced composite materials, due to their homogeneous and isotropic structure, mechanics of the composites are much more sophisticated than that of traditional materials [40].

Fiber reinforced composite materials can be analyzed in two distinct levels: (i) macromechanical analysis and (ii) micromechanical analysis. These terms can be explained as follow.

Micromechanics: The interactions of the components is microscopic level at mechanical analysis. This study is usually conducted by means of a mathematical model defining the response of each component material.

Macromechanics: In this analysis, material is assumed homogeneous. Mechanical analysis of the interactions of the components and their effects of interactions on the overall response quantities of the laminate are investigated in macroscopic level.

At the laminate level, the macromechanical analysis is utilized in the form of lamination theory to analyze whole behaviour as a function of lamina properties and stacking sequence [45].

4.1 Classical Laminated Plate Theory

Classical laminated plate theory is applied to define mechanical behaviour of laminated composites. This theory is only used in the following assumptions

1. Each lamina is homogeneous and orthotropic.
2. Each lamina is elastic and perfectly bounded each other.
3. The laminated composite is thin and the thickness of composite plate are much lesser than its edge dimensions.
4. The loadings are only implemented in the laminate's plane and the laminated composite (except for their edges) is subjected to plane stress ($\sigma_z = \tau_{xz} = \tau_{yz} = 0$).
5. Displacements are small contrast with the thickness of the laminate and they are continuous throughout the laminate.
6. In plane displacements in the x and y directions are linear functions of z .
7. Transverse shear strains (γ_{xz} and γ_{yz}) are ignorable because a line straight and perpendicular to the middle surface preserves state throughout deformation.

Considered thin laminated composite plate in this thesis is shown in Figure 4.1. Global coordinates of the layered material are defined x , y and z . A layer-wise principal material coordinate system is indicated by 1, 2, 3 and fiber direction is oriented at angle θ . Representation of laminate convention for the n -layered structure with total thickness h is given in Figure 4.2.

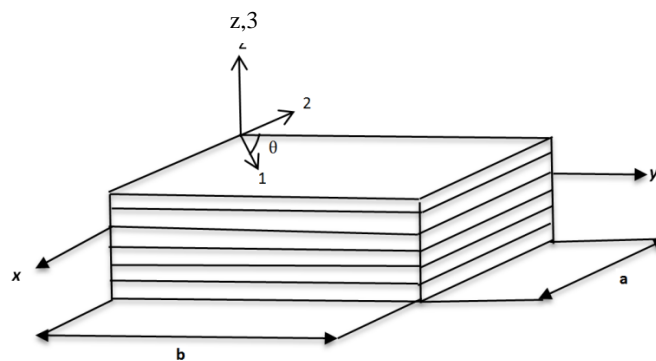


Figure 4.1 : A thin fiber-reinforced laminated composite.

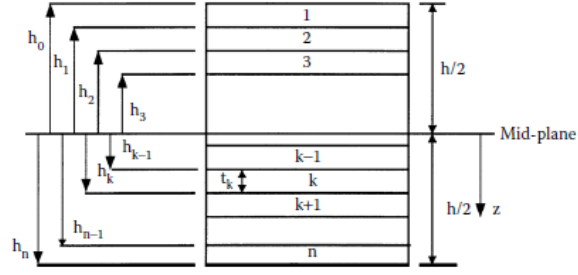


Figure 4.2 : Coordinate locations of plies in a laminate [43].

The strains at any point in the laminate to the reference plane can be written as

$$\begin{bmatrix} \varepsilon_x \\ \varepsilon_y \\ \gamma_s \end{bmatrix} = \begin{bmatrix} \varepsilon_x^o \\ \varepsilon_y^o \\ \gamma_s^o \end{bmatrix} + z \begin{bmatrix} \kappa_x \\ \kappa_y \\ \kappa_s \end{bmatrix} \quad (4.1)$$

The stress-strain relationship for the k -th layer of a laminated composite plate considering the Classical Laminated Plate Theory can be written in the following form

$$\begin{bmatrix} \sigma_x \\ \sigma_y \\ \sigma_{xy} \end{bmatrix}_k = \begin{bmatrix} \bar{Q}_{11} & \bar{Q}_{12} & \bar{Q}_{16} \\ \bar{Q}_{12} & \bar{Q}_{22} & \bar{Q}_{26} \\ \bar{Q}_{16} & \bar{Q}_{26} & \bar{Q}_{66} \end{bmatrix}_k \left(\begin{bmatrix} \varepsilon_x^o \\ \varepsilon_y^o \\ \varepsilon_{xy}^o \end{bmatrix} + z \begin{bmatrix} \kappa_x \\ \kappa_y \\ \kappa_{xy} \end{bmatrix} \right)_k \quad (4.2)$$

where $[\bar{Q}_{ij}]_k$ are the in plane elements of the transformed reduced stiffness matrix under plane stress condition, $[\varepsilon^o]$ is the mid-plane strains, $[\kappa]$ is curvatures, respectively.

The elements of transformed reduced stiffness matrix $[\bar{Q}_{ij}]$ can be expressed as in the following form

$$\bar{Q}_{11} = Q_{11}c^4 + Q_{22}s^4 + 2(Q_{12} + 2Q_{66})s^2c^2 \quad (4.3)$$

$$\bar{Q}_{12} = (Q_{11} + Q_{22} - 4Q_{66})s^2c^2 + Q_{12}(c^4 + s^4) \quad (4.4)$$

$$\bar{Q}_{22} = Q_{11}s^4 + Q_{22}c^4 + 2(Q_{12} + 2Q_{66})s^2c^2 \quad (4.5)$$

$$\bar{Q}_{16} = (Q_{11} - Q_{12} - 2Q_{66})sc^3 - (Q_{22} - Q_{12} - 2Q_{66})s^3c \quad (4.6)$$

$$\bar{Q}_{26} = (Q_{11} - Q_{12} - 2Q_{66})cs^3 - (Q_{22} - Q_{12} - 2Q_{66})sc^3 \quad (4.7)$$

$$\bar{Q}_{66} = (Q_{11} + Q_{22} - 2Q_{12} - 2Q_{66})s^2c^2 + Q_{66}(c^4 + s^4) \quad (4.8)$$

where stiffness matrix quantities $[Q_{ij}]$ are

$$Q_{11} = \frac{E_1}{1 - \nu_{21}\nu_{12}} \quad (4.9)$$

$$Q_{12} = \frac{\nu_{12}E_2}{1 - \nu_{21}\nu_{12}} \quad (4.10)$$

$$Q_{22} = \frac{E_2}{1 - \nu_{21}\nu_{12}} \quad (4.11)$$

$$Q_{66} = G_{12} \quad (4.12)$$

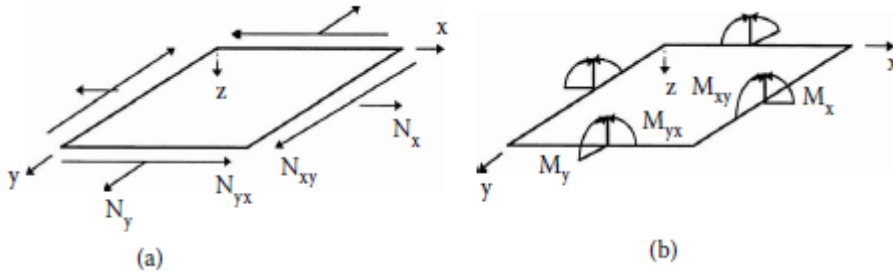


Figure 4. 3 : Resultant forces and moments on a laminate [43].

Applied normal force resultants N_x, N_y , shear force resultant N_{xy} (per unit width) and moment resultants M_x, M_y and M_{xy} on a laminate (Fig. 4.3) have the following relations:

$$\begin{bmatrix} N_x \\ N_y \\ N_{xy} \end{bmatrix} = \begin{bmatrix} A_{11} & A_{12} & A_{16} \\ A_{12} & A_{22} & A_{26} \\ A_{16} & A_{26} & A_{66} \end{bmatrix} \begin{bmatrix} \varepsilon_x^0 \\ \varepsilon_y^0 \\ \gamma_{xy}^0 \end{bmatrix} + \begin{bmatrix} B_{11} & B_{12} & B_{16} \\ B_{12} & B_{22} & B_{26} \\ B_{16} & B_{26} & B_{66} \end{bmatrix} \begin{bmatrix} \kappa_x \\ \kappa_y \\ \kappa_{xy} \end{bmatrix} \quad (3.13)$$

$$\begin{bmatrix} M_x \\ M_y \\ M_{xy} \end{bmatrix} = \begin{bmatrix} B_{11} & B_{12} & B_{16} \\ B_{12} & B_{22} & B_{26} \\ B_{16} & B_{26} & B_{66} \end{bmatrix} \begin{bmatrix} \varepsilon_x^0 \\ \varepsilon_y^0 \\ \gamma_{xy}^0 \end{bmatrix} + \begin{bmatrix} D_{11} & D_{12} & D_{16} \\ D_{12} & D_{22} & D_{26} \\ D_{16} & D_{26} & D_{66} \end{bmatrix} \begin{bmatrix} \kappa_x \\ \kappa_y \\ \kappa_{xy} \end{bmatrix} \quad (3.14)$$

The matrices [A], [B] and [D] specified in Equations 3.13 and 3.14 can be defined as

$$A_{ij} = \sum_{k=1}^n [(\bar{Q}_{ij})]_k (h_k - h_{k-1}), \quad i, j = 1, 2, 6 \quad (3.15)$$

$$B_{ij} = \frac{1}{2} \sum_{k=1}^n [(\bar{Q}_{ij})]_k (h_k^2 - h_{k-1}^2), \quad i, j = 1, 2, 6 \quad (3.16)$$

$$D_{ij} = \frac{1}{3} \sum_{k=1}^n [(\bar{Q}_{ij})]_k (h_k^3 - h_{k-1}^3), \quad i, j = 1, 2, 6 \quad (3.17)$$

The [A] matrix is extensional stiffness regarding in-plane forces to the in-plane strains, [B] matrix is coupling stiffness regarding forces and mid-plane strains, moments and mid-plane curvatures and [D] matrix is bending stiffness regarding moments and curvatures [43].

Now, stresses and strain expressions based on Classical Laminated Plate Theory can be expressed by local coordinate system (1, 2). The relation between the local and global stresses in an angled lamina can be written as in the following form:

$$\begin{bmatrix} \sigma_1 \\ \sigma_2 \\ \sigma_{12} \end{bmatrix} = [T] \begin{bmatrix} \sigma_x \\ \sigma_y \\ \sigma_{xy} \end{bmatrix} \quad (3.18)$$

Similarly, the local and global strains are also related as follows

$$\begin{bmatrix} \varepsilon_1 \\ \varepsilon_2 \\ \varepsilon_{12} \end{bmatrix} = [R][T][R]^{-1} \begin{bmatrix} \varepsilon_x \\ \varepsilon_y \\ \varepsilon_{xy} \end{bmatrix} \quad (3.19)$$

where

$$[R] = \begin{bmatrix} 1 & 0 & 0 \\ 0 & 1 & 0 \\ 0 & 0 & 2 \end{bmatrix} \quad (3.20)$$

and $[T]$ transform matrix,

$$[T] = \begin{bmatrix} c^2 & s^2 & 2sc \\ s^2 & c^2 & -2sc \\ -sc & sc & c^2 - s^2 \end{bmatrix} \quad c = \cos \theta, \quad s = \sin \theta \quad (3.21)$$

4.2 Stresses of the Type III and Type V composite pressure vessels

Cylindrical part of the Type III tank are considered composed of isotropic metallic liner and orthotropic composite layers. Type V tank are also considered only consist of orthotropic composite layers. The laminated composite pressure vessel having radius of “ r_0 ” is subjected to the internal pressure “ p ”. The force resultants, calculated via considerations of static equilibrium [46], are

$$N_x = \frac{1}{2}pr \quad N_y = pr \quad N_{xy} = 0 \quad (4.22)$$

For Type III pressure vessel, only membrane effects are considered, but also the stress in metallic liner and composite is related to the stiffness of each material. It is assumed that strain for the composite and metallic liner is the same. Therefore, in the Type III

analysis, the stiffness of both materials are considered. With this straightforward approach, it can be seen that an $[A]$ matrix including the stiffness of the metal liner and the composite is constructed. By using $[A]$ matrix, the strains occurred because of the loading in the cylinder, stresses in the liner and composite can be calculated from these strains [24].

$$A_{ij} = \sum_{k=1}^n [(\bar{Q}_{ij})_k (h_k - h_{k-1}) + [Q_L] t_L \quad (4.23)$$

Unlike equation 4.15, in the Eq. 4.23 where $[Q_L]$ is stiffness matrix of the metallic liner and t_L is the thickness of the liner. In the Type V analysis, due to be $t_L = 0$, $[A]$ matrix is calculated as 4.15. By using loading, the strains and $[A]^{-1}$ can be calculated from [24]. Eq. (4.24 and 4.25)

$$\begin{bmatrix} \varepsilon_x \\ \varepsilon_y \\ \gamma_{xy} \end{bmatrix} = [A]^{-1} \begin{bmatrix} PR/2 \\ PR \\ 0 \end{bmatrix} \quad (4.24)$$

$$[A]^{-1} = \begin{bmatrix} a_{11} & a_{12} & a_{16} \\ a_{12} & a_{22} & a_{26} \\ a_{16} & a_{26} & a_{66} \end{bmatrix} \quad (4.25)$$

After the obtaining strains for laminates, using stress-strain relationships stress at the liner and each laminate can be determined given [24] by Eq. (4.26) and (4.27)

$$\begin{bmatrix} \sigma_x \\ \sigma_y \\ \tau_{xy} \end{bmatrix} = [Q_L] \begin{bmatrix} \varepsilon_x \\ \varepsilon_y \\ \gamma_{xy} \end{bmatrix} \quad (4.26)$$

$$\begin{bmatrix} \sigma_x \\ \sigma_y \\ \tau_{xy} \end{bmatrix} = [\bar{Q}]^{(k)} \begin{bmatrix} \varepsilon_x \\ \varepsilon_y \\ \gamma_{xy} \end{bmatrix} \quad (4.27)$$

The hoop rigidity ($\bar{E}_y H$) and areal mass density (ρ_s) of the cylindrical composite pressure vessels can be calculated by Eq. (4.28) and (4.29) [46].

$$\bar{E}_y = \frac{1}{a_{22} H} \quad (4.28)$$

$$\rho_s = \int_{-H/2}^{H/2} \rho dz = \sum_{n=1}^N [\rho_f V^{(n)} + \rho_m (1 - V^{(n)})] h^{(n)} \quad (4.29)$$

where H is the total thickness of the laminate, ρ_f and ρ_m are the densities of the fiber and matrix, $V^{(n)}$ is the fiber volume fractions, $h^{(n)}$ is the thicknesses of the each ply and N is the number of plies [46].

4.3 Failure Analysis in Pressure Vessels

The inability of the structure to carry the applied loads can be defined as failure. “Failure causes a load redistribution within the structure, a permanent deformation, or some other evidence that load levels have become excessive” [47]. The main reasons of the failure process are: (i) improper selection of material, (ii) inadequate design process, (iii) insufficient fabrication procedures and (iv) variation of service conditions.

In order to predict the failure loads for a given mechanical and environmental conditions, many researchers have studied to introduce the formulations modeling the failure phenomenon. Most widely used failure theories for isotropic and an-isotropic structures are as follows

4.3.1 Isotropic cases:

Maximum Shear Strain Energy (Von-Mises) :

Assuming the principle stresses $\sigma_1 \geq \sigma_2 \geq \sigma_3$, σ_{yield} is the yield stress in simple tension, the theory states that failure occurs if the following equality is valid

$$(\sigma_1 - \sigma_2)^2 + (\sigma_2 - \sigma_3)^2 + (\sigma_3 - \sigma_1)^2 = 2\sigma_{yield}^2 \quad (4.30)$$

4.3.1 An-isotropic cases:

a) Tsai-Wu Tensor Failure Criterion

According to the theory assumption, failure occurs when the following expression is valid

$$F_1\sigma_1 + F_2\sigma_2 + F_{11}\sigma_1^2 + F_{22}\sigma_2^2 + F_{66}\tau_{12}^2 + 2F_{12}\sigma_1\sigma_2 = 1 \quad (4.31)$$

where F_{12} can be determined with only a biaxial tension test. For calculating the value of F_{12} an empirical expression is suggested as [48]

$$F_1 = \frac{1}{(\sigma_1^T)_{ult}} + \frac{1}{(\sigma_1^C)_{ult}} \quad F_{11} = -\frac{1}{(\sigma_1^T)_{ult}(\sigma_1^C)_{ult}} \quad (4.32)$$

$$F_2 = \frac{1}{(\sigma_2^T)_{ult}} + \frac{1}{(\sigma_2^C)_{ult}} \quad F_{22} = -\frac{1}{(\sigma_2^T)_{ult}(\sigma_2^C)_{ult}} \quad (4.33)$$

$$F_{12} = -\frac{1}{2}\sqrt{F_{11}F_{22}} \quad F_{66} = \frac{1}{(\tau_{12}^F)_{ult}^2} \quad (4.34)$$

b) Hashin-Rotem Criterion

This criterion involves two failure mechanisms as fibre failure and matrix failure, distinguishing between tension and compression [49].

Fibre failure in tension ($\sigma_1 > 0$)

$$\sigma_1 = (\sigma_1^T)_{ult} \quad (4.35)$$

Fibre failure in compression: ($\sigma_1 < 0$)

$$-\sigma_1 = (\sigma_1^C)_{ult} \quad (4.36)$$

Matrix failure in tension: ($\sigma_2 > 0$)

$$\left(\frac{\sigma_1}{(\sigma_2^T)_{ult}}\right)^2 + \left(\frac{\tau_{12}}{(\tau_{12})_{ult}}\right)^2 = 1 \quad (4.37)$$

Matrix failure in tension: ($\sigma_2 < 0$)

$$\left(\frac{\sigma_2}{(\sigma_2^C)_{ult}}\right)^2 + \left(\frac{\tau_{12}}{(\tau_{12})_{ult}}\right)^2 = 1 \quad (4.38)$$

c) The Maximum Stress Theory:

The maximum stress first ply failure criterion based on the assumption that failure is occurred if the σ_1 , σ_{12} and τ_{12} reach the corresponding ultimate strength parameters of materials. There are three possible modes of failure comparing the stress components of the ply with tensile, compression and shear ultimate values.[64]

$$\sigma_1 \leq (\sigma_1^T)_{ult} \quad , \quad \sigma_2 \leq (\sigma_2^T)_{ult} \quad \text{if} \quad \sigma_1 > 0, \sigma_2 > 0 \quad (4.39)$$

$$|\sigma_1| \leq (\sigma_1^C)_{ult} \quad , \quad |\sigma_2| \leq (\sigma_2^C)_{ult} \quad \text{if} \quad \sigma_1 < 0, \sigma_2 < 0 \quad (4.40)$$

$$|\tau_{12}| \leq (\tau_{12})_{ult} \quad (4.41)$$

5. OPTIMIZATION

Optimization can be identified as mathematical process used to form the best design or favorable designs by minimizing or maximizing defined single or multi objectives that fulfill all the constraints. Optimization is frequently used in engineering problems such as weight, cost, vibration, buckling and failure. In such problems, single and multi objective optimization approaches are utilized to obtain desired design of structure. In single objective optimization approach, design and optimization problem comprise of a single objective function, constraints and bounds. Nevertheless, the design and optimization of the engineering structures need to be maximized and / or minimized often conflicting more than one objectives, simultaneously [50]. In this situation, multi-objective approach is used and Pareto optimal solutions are gained. In this approach, it is not possible to obtain the best solution for all objectives, thus only one solution is selected from the set of solutions for practical engineering usage [46].

As design and optimization problems of laminated composites include complicated, highly nonlinear functions, they are unsolvable by the traditional optimization methods. In this situation, the use of stochastic optimization methods such as DE, NM, SA and GA are preferred.

MATHEMATICA is one of the crucial commercial softwares that can be used to solve the design and optimization problems for composites. The software includes stochastic methods Differential Evolution (DE), Nelder Mead (NM), Random Search (RS) and Simulated Annealing (SA) for solving optimization problems. All of these methods are used in the design and optimization of composite structures by researchers.

5.1 Single Objective Optimization

Single objective optimization approach comprises of objective function, design variables, constraints and bounds of constraints. In this study, the problems that are solved using single-objective optimization approach are expressed as follows

$$\text{minimize} \quad f(\theta_1, \theta_2, \dots, \theta_n)$$

$$\text{such that} \quad h_i(\theta_1, \theta_2, \dots, \theta_n) \geq 0 \quad i = 1, 2, \dots, r$$

$$g_j(\theta_1, \theta_2, \dots, \theta_n) = 0 \quad j = 1, 2, \dots, m$$

$$\theta^L \leq \theta_1, \theta_2, \dots, \theta_n \leq \theta^U$$

where f is objective function, $\theta_1, \theta_2, \dots, \theta_n$ are the design variables and h, g are the constraints of the problem. Here, θ^L and θ^U show lower and upper bounds. In design and optimization of composite structure problems; stiffness, mass, strength, displacements, thickness, vibration frequencies, buckling loads, residual stresses, cost and weight are utilized as objective functions [51]. In this thesis, fundamental frequency is taken as objective function of the single-objective optimization problems.

5.2 Multi Objective Optimization

A multi-objective optimization problem can be expressed as follows:

$$\text{minimize} \quad f_1(\theta_1, \theta_2, \dots, \theta_n), f_2(\theta_1, \theta_2, \dots, \theta_n), \dots, f_n(\theta_1, \theta_2, \dots, \theta_n)$$

$$\text{such that} \quad h_i(\theta_1, \theta_2, \dots, \theta_n) \geq 0 \quad i = 1, 2, \dots, r$$

$$g_j(\theta_1, \theta_2, \dots, \theta_n) = 0 \quad j = 1, 2, \dots, m$$

$$\theta^L \leq \theta_1, \theta_2, \dots, \theta_n \leq \theta^U$$

where f_1, f_2, \dots, f_n denote the objective functions to be minimized simultaneously [52].

On the contrary to the traditional multi objective optimization approach, the usage of penalty function formulation may be appropriate because of its advantage of turning constrained optimization problems into the unconstrained ones and thanks to this, it can be applied to the problem by any of the unconstrained methods. In this thesis, penalty approach based on multi objective optimization is considered to maximize the fundamental frequency and minimize the cost, simultaneously.

5.3 Stochastic Optimization Algorithms

Optimization methods can be categorized as traditional and non-traditional. Traditional methods, such as Lagrange Multipliers and Constrained Variation are analytical and find the optimum solution of only continuous and differentiable functions. Because composite design problems usually have discrete search spaces, the traditional optimization methods can not be utilized. In these cases, the usage of stochastic optimization methods such as Simulated Annealing (SA), Genetic Algorithms (GA), Differential Evolution (DE) and Nelder-Mead (NM) are appropriate. A detailed discussion of different optimization methods is expressed in [52] for general application of engineering and in Gurdal et al.[51] for composite design problems. In this thesis, DE, NM, RS and SA methods are used for defined optimizations problems of laminated composites and steps of the algorithms are briefly explained in the following subsections. Related parameters of the algorithms are listed in Tables 5.1 used in adjusting the options correctly.

5.3.1 Differential Evolution Algorithm

Differential Evolution (DE) is a stochastic optimization method which permits alternative solutions for some of the complex composite design and optimization problems such as increasing frequency and frequency separation and obtaining lightweight design. Differential Evolution algorithm includes the following main stages: initialization, mutation, crossover and selection as shown in Figure 5.1. The optimum results of the algorithm change with the parameters: scaling factor, crossover and population size. Detail description of the DE can be found in [53]. DE always considers a population of solutions instead of a single solution at each iteration and is also computationally expensive. It is relatively robust and efficient in finding global

optimum of the objective function. However, it is not guaranteed to find the global optima.

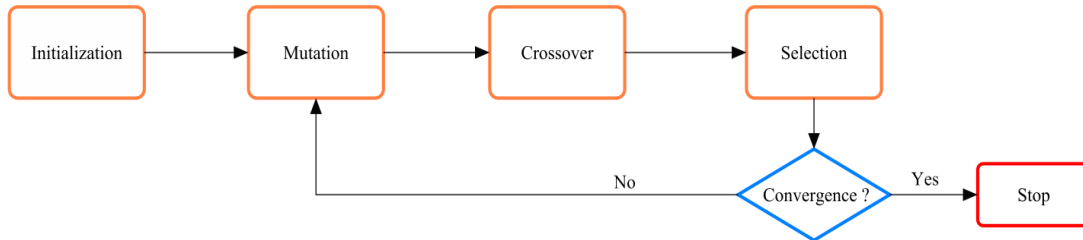


Figure 5.1 : Flowchart of the DE algorithm [58].

The first step of DE optimization process is Initialization. There are several approaches to populate the initial generation. Random generation is widely used approach for solution. In this step, the algorithm maintains a population of r points, $\{x_1, x_2, \dots, x_k, \dots, x_r\}$, where typically $r \gg m$, with m being the number of variables. In second step, Mutation, a genetic operator that maintains the genetic variety from one generation of a population to the next generation. In mutation process, the solution can be different from the previous solution and thus a better solution can be gained. In third step, Crossover is used to obtain a richer population. Genetic diversity is encouraged by the interchange of genetic material between chromosomes and then, the gene strings of the related chromosomes are split at the same point in the parents and two parents create a child. Finally, the last step selection is applied and the new individual is added to the new population [51, 54, 55].

5.3.2 Nelder Mead Algorithm

The Nelder–Mead (simplex search) algorithm is a traditional local search method designed by Nelder and Mead (1965) firstly for unconstrained optimization problem [56]. Although Nelder–Mead is not a global optimization algorithm, it is inclined to work fairly well for problems which do not have many local minima in practical usage. The adjustment of the algorithm options is controlled by four basic procedures: reflection, expansion, contraction and shrinkage. One of the characteristic properties of the algorithm is that NM often gives considerable improvements in the first few iterations and rapidly generates quite adequate results. Moreover, the method usually needs only one or two function evaluations per iteration, apart from shrink

transformations, which are notably rare in practice. This is very important in applications that each function evaluation is very expensive or time-consuming. Furthermore, the simplex can vary its orientation, size and shape to adapt itself to the local contour of the objective function, hence NM has high flexibility in exploring difficult domains [57]. The main steps of the algorithm are given in Figure 5.2.

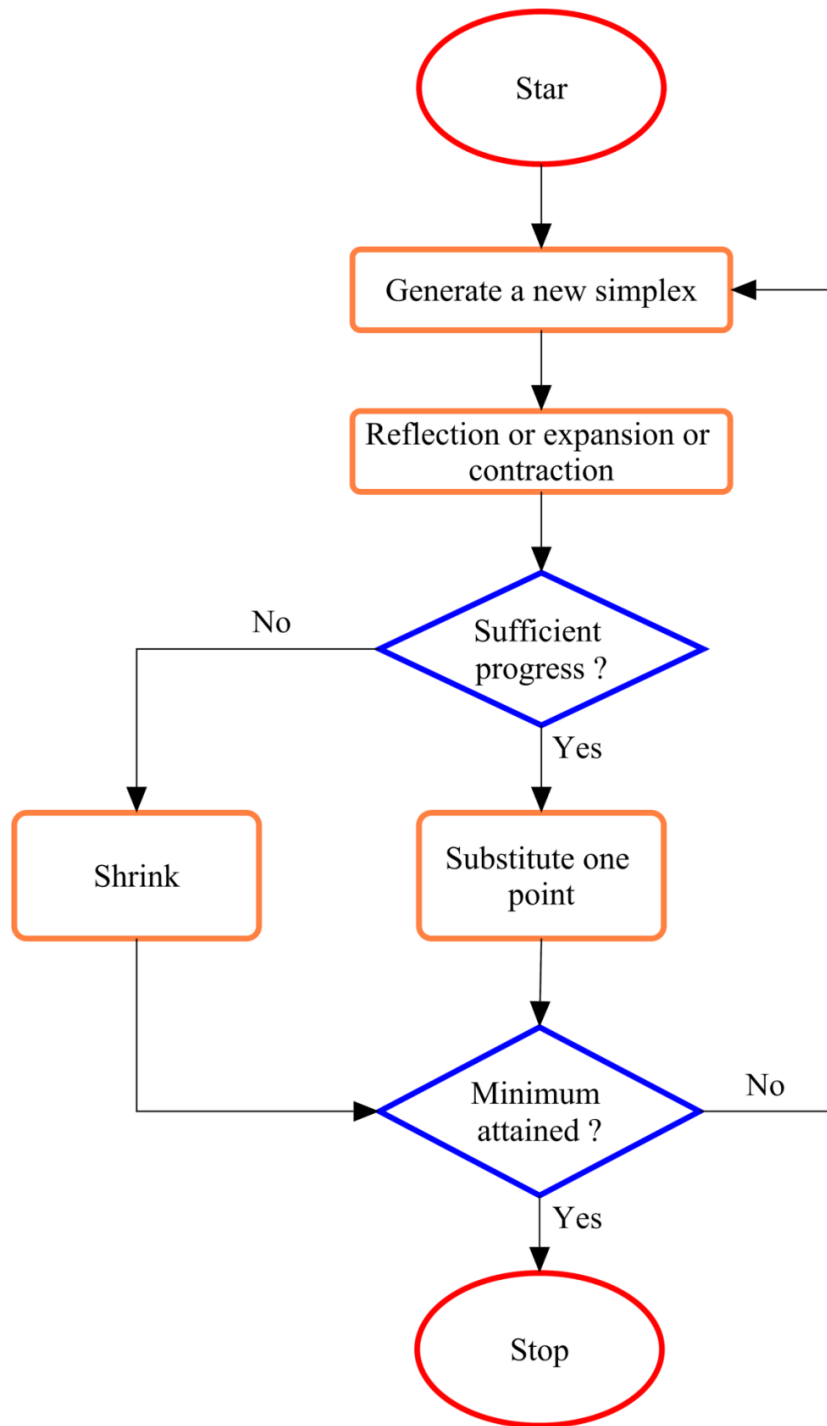


Figure 5.2 : Flowchart of the NM algorithm [59].

5.3.3 Simulated Annealing Algorithm

One of the most popular random search methods is SA. It is based on the physical process of annealing, that a metal object is warmed up to a high temperature and permit to cool slowly. The melting process lets the atomic structure of the material to pass to a lower energy condition, hence that becoming a tougher material. From the view point of optimization, in SA algorithm, annealing process lets the structure to get away from a local minimum, and to explore and settle on a better global optimum point. The main advantage of SA is that that it enables to solve various optimization problems such as continuous, discrete or mixed-integer. In the working phase of this method, a new point is randomly produced at each iteration and when all stopping criteria are fulfilled the algorithm stops. Optimization methods options are given in Table 5.1.

Table 5.1 : Three optimization methods options.

Options Name	DE	NM	SA
CrossProbability	0.5	-	-
RandomSeed	0	5/1/2/5	0
ScalingFactor	0.6	-	-
SearchPoints	-	-	1000
Tolerance	0.001	0.001	0.001
ContractRatio	-	0.5	-
ExpandRatio	-	2.0	-
ReflectRatio	-	1.0	-
ShrinkRatio	-	0.5	-
LevelIterations	-	-	50
PerturbationScale	-	-	1.0

The space of the new point from the current point or the extent of the search is based on Boltzmann's probability distribution. The distribution implies the energy of a system in thermal equilibrium at temperature "T". Boltzmann's probability distribution can be expressed in the following form [52] :

$$P(E) = e^{-E/kT} \quad (4.1)$$

where $P(E)$ represents the probability of achieving the energy level E , k is the Boltzmann's constant, and T is temperature. In order to follow the procedure of the algorithm easily, the flowchart of a SA algorithm is presented in Figure 5.3.

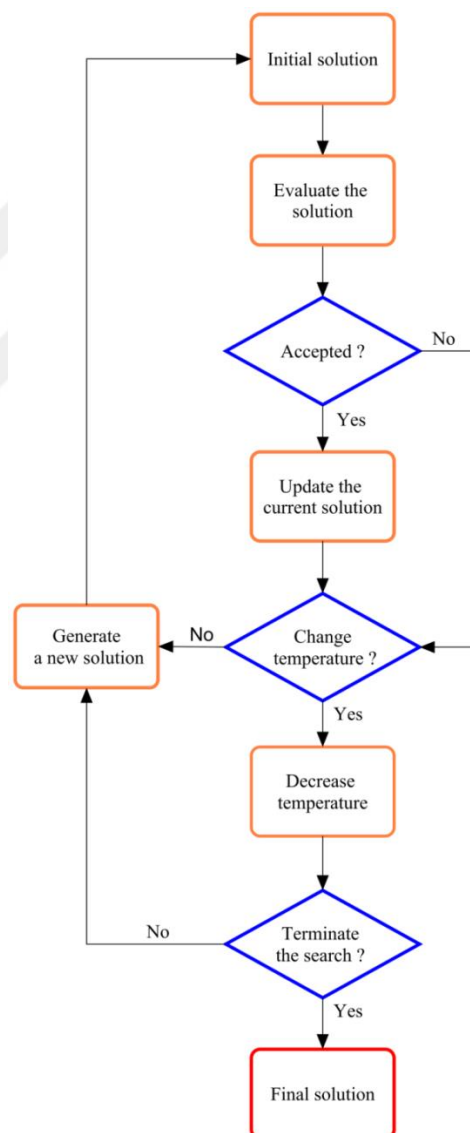


Figure 5.3 : Flowchart of the SA algorithm [60].



6. VERIFICATION PROBLEMS

In design problems of the pressure vessels, it is crucial to be able to predict the burst pressure. There are three main steps for design and optimization of the composite vessels: (i) to determine the burst pressure of the vessels by proposed lamination and failure theories, (ii) to define mathematical optimization problem including objective function, constraints and design variables and (iii) to select appropriate optimization algorithms.

Various studies in the literature have been considered as problems in this section in order to confirm the burst pressure predictions and the appropriateness of the optimization algorithms. Additionally, in the prediction of burst pressure and stacking optimization problems, it is focused on cylindrical parts of the pressure vessels. In these problems, two types of tanks are considered as: (i) composed of composite plies and aluminum liner (Type III) and (ii) just composite plies (Type V) (see Figs. 6.1 and 6.2). The stress components of composite laminates are analyzed based on classical laminate theory and failure criteria given in Chapter 3.

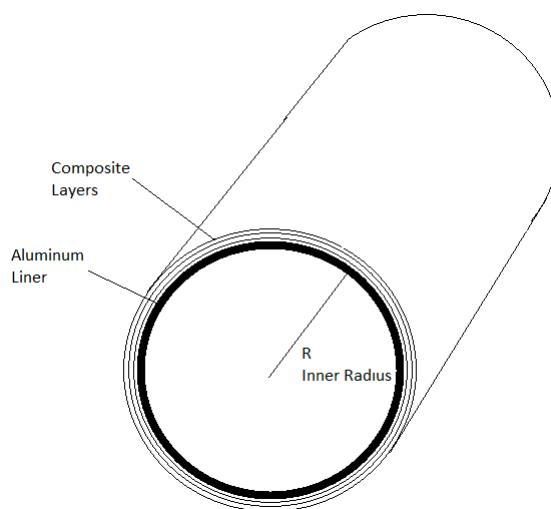


Figure 6.1: Cylindrical part of the Type III pressure vessel.

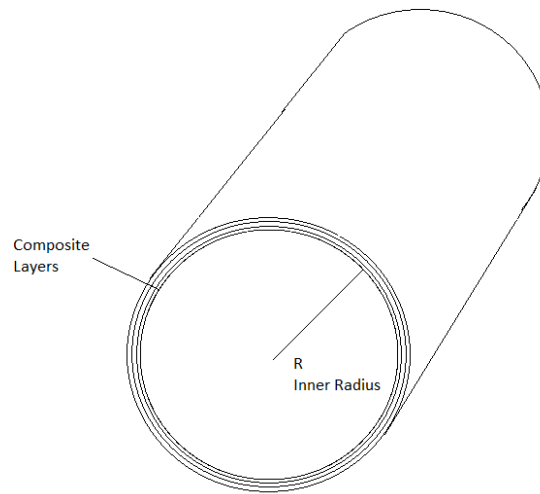


Figure 6.2: Cylindrical part of the Type V pressure vessel.

In the present chapter, composite pressure vessels are considered as composed of cylindrical plies. For Type III hydrogen storage tanks, aluminum liner have been considered as in Chapter 4. Table 6.1 shows that the verification studies including detailed information in Chapter 6.

Table 6.1 : Verifications Studies.

Verification Studies	Study	Material	Method
V1	Comparison of Burst Pressure, Areal Mass Density and Hoop Rigidity for Type V Pressure Vessel	Graphite /Epoxy	Classical Laminated Plate Theory (CLPT) Tsai- Wu Failure Criterion
V2	Design and Optimization of the Cylindrical Part of the Type V Composite Pressure Vessel by Using DE, SA and NM Methods	Graphite /Epoxy	Classical Laminated Plate Theory (CLPT) Tsai- Wu Failure Criterion Differential Evolution Simulated Annealing Nelder Mead
V3	Comparison of the Burst Pressure Prediction with Experimental Study for Type V Pressure Vessel	T700 Carbon /Epoxy	Classical Laminated Plate Theory (CLPT) Tsai- Wu Failure Criterion
V4	Comparison of the Burst Pressure Prediction by using Tsai – Wu and Maximum Stress failure Criteria for Type III Pressure Vessel	T6061 Aluminum T700 Carbon /Epoxy	Classical Laminated Plate Theory (CLPT) Tsai- Wu Failure Criterion Maximum Stress Criterion
V5	Comparison of the Burst Pressure Prediction with Experimental Study for Type III Pressure Vessel	T6061 Aluminum Carbon/ Epoxy	Classical Laminated Plate Theory (CLPT) Tsai- Wu Failure Criterion Maximum Stress Failure Criterion Hashin-Rotem Failure Criterion

6.1 Problem V1.

In the problem V1, cylindrical pressure vessels (tanks) composed of the symmetric Graphite fiber reinforced Epoxy composites are considered. The main purpose of the problem V1 is to compare the burst pressure, areal mass density and hoop rigidity calculations with the results given in the study [46]. Burst pressure of the tanks have been determined by using Tsai-Wu first ply failure criterion. The thickness of each composite ply is 0.45 mm. The radius of the pressure vessels R are 1 meter. The tanks are subjected to an internal pressure “ p ”. The mechanical properties and strength values of Graphite/Epoxy composite are given in Tables 6.2 and 6.3. There are 10 design cases (a- j) which have been solved by Pelletier and Vel [46]. Results of these cases are also given in Tables 6.4 and 6.5.

Table 6.2 : Mechanical properties of Graphite/Epoxy composite materials [46].

$E_1(\text{GPa})$	$E_2(\text{GPa})$	$G_{12}(\text{GPa})$	ν_{12}	ν_{23}
165.862	9.79619	4.96043	0.275	0.49

Table 6.3 : Strength parameters of Graphite/Epoxy composite materials [46].

$\sigma_{1\text{ult}}^T(\text{MPa})$	$\sigma_{1\text{ult}}^C(\text{MPa})$	$\sigma_{2\text{ult}}^T(\text{MPa})$	$\sigma_{2\text{ult}}^C(\text{MPa})$	$\tau_{12\text{ult}}(\text{MPa})$
1811.25	-1064.35	94.0562	-220.073	80.6954

Table 6.4 : Comparison results of the present thesis and the study by Pelletier and Vel [46] for burst pressure calculations.

(Note: The present study considers problem V1)

Design Cases	Orientations	P_{burst} pressure (MPa) [46]	P_{burst} pressure [Present Study] (MPa)
a	[90] _s	0.754	0.754
b	[90/-75/60/90] _s	0.954	0.954
c	[0/90] _{3s}	3.512	3.512
d	[45/-60/60/-60] _s	3.831	3.831
e	[90 ₃ /15/-30/90] _s	5.208	5.208
f	[90] _{10s}	1.886	1.886
g	[0/75/90 ₃ /-45/90] _{3s}	5.598	5.598
h	[90 ₄ /0/90 ₃ /0] _s	7.433	7.433
i	[90/30/90/-30/15/90 ₃ /-15/90] _s	9.597	9.597
j	[90 ₅ /0/90 ₂ /0 ₂] _s	9.476	9.476

Table 6.5 : Comparison results of the present thesis and the study by Pelletier and Vel [46] for hoop rigidity and areal mass density.
(Note: The present study considers problem V1)

Design Cases	Hoop Rigidity $\bar{E}_y H$ [46]	Hoop Rigidity $\bar{E}_y H$ [Present Study]	Areal Mass Density ρ_s (kg / m ²) [46]	Areal Mass Density ρ_s (kg / m ²) [Present Study]
a	597.102	597.102	5.8734	5.8734
b	479.518	479.518	5.8734	5.8734
c	458.154	458.154	5.8734	5.8734
d	161.089	161.089	5.8734	5.8734
e	617.161	617.161	8.8101	8.8101
f	1492.79	1492.79	14.6835	14.6835
g	1069.48	1069.48	13.2152	13.2152
h	1066.00	1066.00	13.2152	13.2152
i	939.277	939.277	14.6835	14.6835
j	1075.03	1075.03	14.6835	14.6835

The calculated results of the burst pressure, areal mass density and hoop rigidity parameters for cylindrical part of composite pressure vessel have been compared with that of the study by Pelletier and Vel (see Tables 6.4 and 6.5) [46]. The same values have been obtained. Therefore, a usable analytical calculation procedure can be approved for burst pressure relevant to first ply failure theories, areal mass density and hoop rigidity.

6.2 Problem V2.

The problem V2 is about design and optimization for composite Type V pressure vessel at the study given in [46]. Optimization problem has been solved in this thesis by using DE, SA and NM. After solving the problems, the present results have been compared with the results given in the study [46]. Because of the manufacturing constraints, (i) fiber orientation angles are considered in the range of -90 and 90 with 15 degree increments, (ii) the maximum number of lamina layers is 20, (iii) stacking sequences of the plies have been counted as symmetric.

In the study conducted by Pelletier and Vell, there are three objectives to be maximizing the failure pressure P , maximizing the hoop rigidity $E_y H$ and minimizing the areal mass density ρ_s (multiobjective approach). In this thesis, the optimization problem has been introduced based on single objective approach. In this case, objective function has been chosen as the hoop rigidity $E_y H$. The other parameters failure burst pressure (P) and areal mass density ρ_s have been considered as constraints.

The mathematical representation of Problem V2 can be defined as:

Maximize: $E_y H$ (Hoop Rigidity)

Constraints: $\{F_{Tsai-Wu}\} \leq 1$,

$$\rho_s \leq \rho_{\text{sallowable}}$$

$$P \geq P_{\text{allowable}} - 0.2$$

$$\text{Number of layers} = n \in \{8, 12, 18, 20\}$$

$$\theta \in \{-90, -75, -60, -45, -30, -15, 0, 15, 30, 45, 60, 75, 90\},$$

Symmetric & Balance stacking sequences,

$$t_{\text{ply}} = 0.45 \text{ mm}$$

where $F_{Tsai-Wu}$, $\rho_{\text{sallowable}}$, $P_{\text{allowable}}$ and t_{ply} denote failure index at all the layers, maximum areal mass density, minimum allowable burst pressure and thickness of each ply, respectively. The design constraints for optimization problems of the composite Type V pressure vessel design cases (a-j) are listed in Table 6.6.

Table 6.6 : Design constraints used in problem V2.

Design Cases	P_{allowable} (MPa) [46]	ρ_s allowable (kg / m²) [46]	n [46]
a	0.754	5.8734	8
b	0.954	5.8734	8
c	3.512	5.8734	8
d	3.831	5.8734	8
e	5.208	8.8101	12
f	1.886	14.6835	20
g	5.598	13.2152	18
h	7.433	13.2152	18
i	9.597	14.6835	20
j	9.476	14.6835	20

Table 6.7 : Comparison of the results of the Hoop Rigidity by using DE, SA and NM.

Design	Hoop Rigidity (E_y H) (M N/m)			
	DE [Present]	SA [Present]	NM [Present]	GA [46]
a	597.102	597.102	597.102	597.102
b	479.519	479.519	479.519	479.518
c	458.155	458.155	458.155	458.154
d	161.089	161.089	339.217	161.089
e	617.162	617.162	617.162	617.161
f	1492.79	1450.97	1318.85	1492.79
g	1069.48	1075.39	1070.1	1069.48
h	1066.00	1066.00	1066.00	1066.00
i	950.276	997.756	945.385	939.277
j	1075.03	1074.5	1075.03	1075.03

Table 6.8 : Comparison of the results of the stacking sequences design by using DE, SA and NM methods.

Stacking Sequences				
	DE [Present]	SA [Present]	NM [Present]	GA [46]
a	[90 ₄] _s	[90 ₄] _s	[90 ₄] _s	[90 ₄] _s
b	[90/-60/75/90] _s	[60/90/-75/90] _s	[-75/90 ₂ /-60] _s	[90/-75/60/90] _s
c	[90/0/90 ₂] _s	[90/0/90 ₂] _s	[90 ₃ /0] _s	[0/90 ₃] _s
d	[60/45/60 ₂] _s	[-45/90 ₂ /30] _s	[-60/75 ₂ /0] _s	[45/-60/60/-60] _s
e	[-15/90/30/90 ₃] _s	[90 ₂ /-30/15/90 ₂] _s	[90 ₂ /-15/90/30/ 90] _s	[90 ₃ /15/-30/90] _s
f	[90 ₁₀] _s	[75/90 ₉] _s	[90 ₃ /-75/ 90/ -15/ 90 ₄] _s	[90 ₁₀] _s
g	[45/90/-75/90 ₃ /0/90 ₂] _s	[90 ₃ /-45/ 90 ₄ /15] _s	[-60/ 90/ 75/ 0/ ±75/ 90 ₃] _s	[0/75/90 ₃ /-45/90 ₃] _s
h	[0/90 ₃ /0/90 ₄] _s	[90 ₅ /0/90 ₂ /0] _s	[90 ₃ / 0/ 90 ₂ / 0/ 90 ₂] _s	[90 ₄ /0/90 ₃ /0] _s
i	[0/90/-15/90 ₄ /-15/90/45] _s	[-75/ 0 ₂ /75/ 90 ₂ /0/-75/90/75] _s	[0/-45/45/ 90 ₃ / 0/ 90/ 75/ -75] _s	[90/30/90/-30/15/90 ₃ / -15/90] _s
j	[90 ₄ /0/90 ₃ /0/90 ₄] _s	[0/±15/90 ₇] _s	[0/90 ₂ /0 ₂ /90 ₅] _s	[90 ₅ /0/90 ₂ /0 ₂] _s

Table 6.9 : Comparison of the results of the areal mass density by using DE, SA and NM.

Areal Mass Density				
ρ_s (kg / m ²)				
Design	DE [Present]	SA [Present]	NM [Present]	GA [46]
a	5.8734	5.8734	5.8734	5.8734
b	5.8734	5.8734	5.8734	5.8734
c	5.8734	5.8734	5.8734	5.8734
d	5.8734	5.8734	5.8734	5.8734
e	8.8101	8.8101	8.8101	8.8101
f	14.6835	14.6835	14.6835	14.6835
g	13.2152	13.2152	13.2152	13.2152
h	13.2152	13.2152	13.2152	13.2152
i	14.6835	14.6835	14.6835	14.6835
j	14.6835	14.6835	14.6835	14.6835

As the results of problem V2; (i) three different algorithms Differential Evolution, Simulated Annealing and Nelder-Mead have been used to solve the optimization problem that studied by [46]. (ii) For some cases, while Differential Evolution, Simulated Annealing and Nelder-Mead algorithms have better performed than Genetic Algorithms, in some cases they have low performance. (Tables 6.7, 6.8, 6.9 and 6.10)

Table 6.10 : Comparison of the results of the burst pressure by using DE, SA and NM.

Design	$P_{burst\ pressure}(MPa)$			
	DE [Present]	SA [Present]	NM [Present]	GA [46]
a	0.754	0.754	0.754	0.754
b	0.954	0.954	0.954	0.954
c	3.512	3.512	3.512	3.512
d	3.835	3.818	3.770	3.831
e	5.208	5.208	5.208	5.208
f	1.886	1.886	1.888	1.886
g	5.600	5.600	5.490	5.598
h	7.437	7.437	7.435	7.433
i	9.596	9.590	9.550	9.597
j	9.476	9.318	9.470	9.476

6.3 Problem V3

In the problem V3, for Type V pressure vessel, it was targeted to see the differences with experimental burst pressure and analytical burst pressure determination of Tsai-Wu failure criterion. The pressure vessel is composed of T700 Carbon/Epoxy carbon reinforced composite plies [61]. Geometrical dimensions of the pressure vessel are 50 mm inner radius, 300 mm Length and 0.125 mm one thickness of one ply of the composite. Material properties have been given (Table 6.11 and 6.12).

Table 6.11 : Mechanical properties of T6061 Al and T700 Carbon/Epoxy composite materials [61].

	$E_1(GPa)$	$E_2(GPa)$	$G_{12}(GPa)$	ν_{12}	ν_{21}
T700 Carbon/Epoxy	142.5	9.79	4.72	0.27	0.018

Table 6.12 : Strength parameters of T700 Carbon/Epoxy composite materials [61].

σ_{1ult}^T (MPa)	σ_{1ult}^C (MPa)	σ_{2ult}^T (MPa)	σ_{2ult}^C (MPa)	τ_{12ult} (MPa)
2193	2457	41.3	206.8	61.28

In Table 6.13, the comparison of the burst pressure predictions based on Tsai-Wu first failure criterion and experimental results for Type V pressure vessels are given. The comparison of three cases shows that the maximum errors between the analytical (present) and experimental results have changed at the range of the 15% and 5%.

Table 6.13 : Comparison of the burst pressure calculations based on numerical and analytical approaches with the experimental one.

Fiber orientation	Burst Pressure Tsai-Wu (Numerical) [61] (MPa)	Burst Pressure (Experimental) [61] (MPa)	Burst Pressures Tsai-Wu [Present Study] (MPa)
[54/-54/54/-54] _s	5.26	5.39	5.49
[54/-54/54/-54/54/-54] _s	7.28	7.6	8.24
[54/-54/54/-54/54/-54/54/-54] _s	9.22	9.61	10.97

6.4 Problem V4

In the Problem V4, the stress and failure indexes of Tsai-Wu and Maximum Stress failure criteria have been computed for Type III Aluminum Carbon Epoxy composite pressure vessel. Material properties have been taken from ref. [24] (see Table 6.14 and 6.15). The internal radius of the tank is 100 mm and the volume is 10 Liter. The other parameters liner thickness and applied pressure are 3 mm and 164.5 MPa, respectively. For Type III tank, it has been considered that the liner and reinforcing materials are Aluminum T6061 and composite T700 Carbon/Epoxy. The main purpose of this problem is to compare failure indexes obtained by the present study and results by Alcantar [24] for Type III pressure vessel.

Table 6.14 : Mechanical properties of T6061 Al and T700 Carbon/Epoxy composite materials [24].

	$E_1(\text{GPa})$	$E_2(\text{GPa})$	$G_{12}(\text{GPa})$	ν_{12}	ν_{23}	$\sigma_{ult} (\text{MPa})$
6061Al	70	70	26.92	0.3	0.3	310
T700 Carbon/Epoxy	181	10.3	5.86	0.28	0.49	-

Table 6.15 : Strength parameters of T700 Carbon/Epoxy composite materials [24].

$\sigma_{1ult}^T(\text{MPa})$	$\sigma_{1ult}^C(\text{MPa})$	$\sigma_{2ult}^T(\text{MPa})$	$\sigma_{2ult}^C(\text{MPa})$	$\tau_{12ult}(\text{MPa})$
2150	2150	298	298	778

Table 6.16 : Results of the Tsai-Wu and Maximum Stress failure indexes.

Burst Pressure (MPa)	Tsai-Wu Failure Index Ref. [24]	Tsai-Wu Failure Index [Present Study]	Maximum Stress Failure Index Ref. [24]	Maximum Stress Failure Index [Present Study]
164.5	0.83	0.85	0.90	1.00
105	0.51	0.35	0.56	0.64

The results of the Problem V4 can be summarized as:

(i) the present failure indexes calculations using Tsai-Wu and Maximum Stress theories have been compared with the results achieved by Finite Element Method (see Table 6.16). It is shown that good agreement between the present and FEM results by Alcantar et al [24] are obtained.

(ii) for Type III pressure vessels, the burst pressure prediction has also been developed by using the stress-strain matrix calculation method given in Alcantar et al [24].

6.5 Problem V5

Stress calculation and determination of the burst pressure according to Classical Laminated Plate Theory and Tsai-Wu failure criterion have been done for Aluminum-Carbon Epoxy pressure vessel (Type III). The burst pressure results have been compared with experimental and Finite Element analysis results by Liu et al [62]. The pressure vessel is composed of T6061 Aluminum liner and T700 Carbon/Epoxy composite plies. Mechanical properties and strength parameters of these materials are given in Table 6.17 and 6.18, respectively.

Table 6.17 : Mechanical properties of T6061 Al and T700 Carbon/Epoxy composite materials [62].

	E_1 (GPa)	E_2 (GPa)	G_{12} (GPa)	ν_{12}	ν_{23}	σ_{yield} (MPa)
6061Al	70	70	26.92	0.3	0.3	246
T700 Carbon/Epoxy	154.1	10.3	5.17	0.28	0.49	-

Table 6.18 : Strength parameters of T700 Carbon/Epoxy composite materials [62].

σ_{1ult}^T (MPa)	σ_{1ult}^C (MPa)	σ_{2ult}^T (MPa)	σ_{2ult}^C (MPa)	τ_{12ult} (MPa)
2500	1250	60	186	85

Geometrical properties for considered Type III pressure vessel have been indicated in Table 6.19.

Table 6.19 : Geometrical Dimensions of the Type-III Pressure Vessel [62].

Internal Radius (mm)	Stacking Sequences (°)	Liner Thickness (mm)	Thickness Of Composite Ply (mm)
44	[90 ₂ , 18.6, -18.6, 90 ₂ , 28.9, -28.9, 90 ₂]	1.8	0.42

Table 6.20 shows comparison results of the calculated burst pressure values that satisfy Tsai-Wu failure criterion constraint with the experimental and Finite Element analysis results. It can be seen that good agreement is reached among them with the maximum error of 10%. Additionally, burst pressure values calculated by using Maximum Stress and Hashin-Rotem failure criterion have predicted with the maximum error of 30 %.

Table 6.20 : Comparison of the burst pressure for Problem V5.

	Tsai-Wu First Ply Failure [Present]	Maximum Stress First Ply Failure [Present]	Hashin- Rotem First Ply Failure [Present]	Finite Element [62]	Experimental [62]
Burst Pressure (Mpa)	90	70	70	99.8	106

It is seen that the predictions made here are based on the first ply failure criteria, however, the progressive failure approach should be used in order to obtain the final ply failure burst pressure. It should also be noted that the use of first ply failure approach provide safer designs during the optimization procedure.



7. OPTIMIZATION PROBLEMS

There are some important issues as structural stability and airtightness to be able to store high-pressure hydrogen gas in the tanks. Therefore, hydrogen storage tanks are generally made up with a load-sharing aluminum or polymer liner and composite wound layers. Type III tank is composite wound with a load-sharing aluminum liner (see Figure 7.1). Type V pressure vessel also composed of a composite cylinder without liner and only composite structure carries all of the stresses of the pressurized gas.

In this Chapter, because of the importance of the structural stability, different design and optimization problems that contain capability of the strength against to internal pressure for Type III and Type V pressure vessels have been solved by using DE, NM and SA methods (see Table 7.1). Classical Laminated Plate Theory (CLPT) have been used to calculate stresses and strains. Tsai-Wu, Hashin Rotem and Maximum Stress failure theories have been selected as constraints to determine the burst pressure of the tanks.

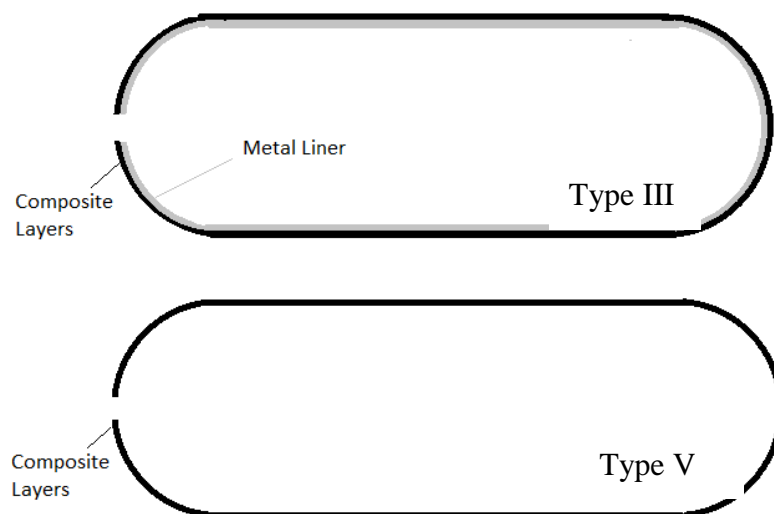


Figure 7.1 : Configuration of the Type III and Type V Pressure Vessel.

Table 7.1 : Optimization Problems.

Prob. No	Aims	Optimization Algorithms	Material	Constraints
1	Optimum Stacking Sequences Design of the Type III Pressure Vessel	DE, SA	. T700 Carbon/Epoxy [62]	$F_{Tsai-Wu} \leq 1$ $F_{Hashin-Rotem} \leq 1$, $F_{Maximum\ Stress} \leq 1$ $\theta \in \text{Integers}$ Symmetric-Balanced $P_{burst} > 170\ \text{MPa}$
2	Optimum Stacking Sequences Design of the Type III Pressure Vessel	DE, SA	. T700 Carbon/Epoxy [62]	$F_{Tsai-Wu} \leq 1$ $F_{Hashin-Rotem} \leq 1$, $F_{Maximum\ Stress} \leq 1$ $\theta \in \text{Integers}$ Symmetric-Balanced $P_{burst} > 150\ \text{MPa}$
3	Minimization of Tsai-Wu Failure Index for Type III Pressure Vessel With Different Ply Thicknesses	DE	. T700 Carbon/Epoxy [62]	$F_{Tsai-Wu} \leq 1$, $-90^0 \leq \theta \leq 90^0$, $P_{burst} > 110\ \text{MPa}$
4	Design and Optimization of Type III Pressure Vessel for Different Carbon/Epoxy Materials	DE	. T700 CARBON/Epoxy [62] . Carbon/ Epoxy (T700s)[24] . Carbon/ Epoxy (IM6/SC1081)[63]	$F_{Tsai-Wu} \leq 1$ $F_{Hashin - Rotem} \leq 1$, $F_{Maximum\ Stress} \leq 1$ $\theta \in \{0,15,45,60,75,90\}$ Symmetric-Balanced $P_{burst} > 35\ \text{MPa}$
5	Stacking Sequences Design of the Cylindrical Composite Pressure Vessel for Different Carbon/ Epoxy Materials	DE	. Carbon/ Epoxy[62] . Carbon/ Epoxy (T700s)[24] . Carbon/ Epoxy (IM6/SC1081)[63]	$F_{Tsai-Wu} \leq 1$ $\theta \in \{0,15,45,60,75,90\}$ Symetric-Balanced $P_{burst} > 35\ \text{MPa}$
6	Stacking Sequences Optimization of Type III Pressure Vessel	DE, SA, NM	. Aluminum T6061 . Carbon/ Epoxy (T700s)[24]	$F_{Tsai-Wu} \leq 1$ $\theta \in \text{Integers}$ Symmetric-Balanced $P_{burst} > 140\ \text{MPa}$

7.1 Definitions for Problems 1, 2 and 3

Two design possibilities can usually be considered for Type III tanks design: (i) with a liner yield, (ii) without yielding of liner. In problem 1,2 and 3, yielding of liner have been assumed as constraint under the internal working pressure of 70 Mpa. In addition to this, it hasn't been taken as a constraint over 70 Mpa.

T6061 Aluminum and carbon reinforced composite materials (T700 Carbon/Epoxy) are used for the tank. Mechanical properties and strength parameters of these materials are given in Tables 7.2 and 7.3, respectively.

Table 7.2 : Mechanical properties of T6061 Al and T700 Carbon/Epoxy composite materials.

	$E_1(\text{GPa})$	$E_2(\text{GPa})$	$G_{12}(\text{GPa})$	ν_{12}	ν_{23}	$\sigma_{yield} \text{ (MPa)}$
6061Al [62]	70	70	26.92	0.3	0.3	246
T700 Carbon/Epoxy[19]	181	10.3	5.17	0.28	0.49	-
T700 Carbon/Epoxy[62]	154.1	10.3	5.17	0.28	0.49	-

Table 7.3 : Strength parameters of T700 Carbon/Epoxy composite materials [62]

$\sigma_{1ult}^T \text{ (MPa)}$	$\sigma_{1ult}^C \text{ (MPa)}$	$\sigma_{2ult}^T \text{ (MPa)}$	$\sigma_{2ult}^C \text{ (MPa)}$	$\tau_{12ult} \text{ (MPa)}$
2500	1250	60	186	85

The second step is design and optimization part: overall procedures for different optimization cases have been summarized briefly.

- Close-end cylindrical section of the Type III tanks have been only considered subjected to high internal pressure “P”.

- It is considered to be constant over the length of the cylinder for inner radius ($R_0 = 44$ mm), thicknesses of the composite layers ($t_{ply} = 0.42$ mm or $t_{ply} = 0.21$ mm) and aluminum liner ($t_{liner} = 1.8$ mm).
- For the optimization problems 1 and 2, three different failure criteria to be interactive, partial-interactive and non-interactive: Tsai-Wu, Hashin Rotem and Maximum Stress have been used as constraints. In optimization problem 3, Tsai-Wu failure criterion is considered only.
- All optimization cases of composite cylindrical tanks have been assumed to be single objective optimization problem.
- Fiber orientation angles $\theta_1, \theta_2, \theta_3, \dots, \theta_n$ and number of layers are selected as the design variables.

Problem 1

In design problem 1, there are two main purposes: (i) to compare the results based on Simulated Annealing and Differential Evolution algorithms and (ii) to propose safety designs of symmetric-balanced stacking sequences over 170 Mpa. The yield of the liner is prohibited at working pressure 70 Mpa. Additionally, Tsai-Wu, Hashin Rotem and Maximum Stress failure indexes F_i of all the layers have been proposed to be less than 1. Thicknesses of the composite layers are 0.42 mm.

Problem 1 can be defined as mathematically:

Minimize: $F_{T[1]}$ (Tsai-Wu Failure Index at first layer)

Constraints: $\{F_{Tsai-Wu}, F_{Hashin-Rotem}, F_{Maximum\ Stress}\} \leq 1, \sigma_{von-Misses} < \sigma_{yield}$

$$-90^0 \leq \{\theta_1, \theta_2, \theta_3, \dots\} \leq 90^0, \{\theta_1, \theta_2, \theta_3, \dots\} \in \text{Integers},$$

$$P_{burst} > 170 \text{ MPa},$$

Symmetric & Balance stacking sequences;

$$[\pm\theta_1/\pm\theta_2/\pm\theta_3/ \dots / \mp\theta_3/\mp\theta_2/\mp\theta_1]$$

$$t_c = 0.42 \text{ mm}, t_{liner} = 1.8 \text{ mm}$$

Problem 2

As different from Problem 1, in design Problem 2, minimum burst pressure constraint is given as 157.5 Mpa. Symmetric and balance stacking sequences design have also been considered. SA and DE are used as optimization method. It is also supposed to be less than 1 for Tsai-Wu, Hashin Rotem and Maximum Stress failure indexes of the all layers. Each thickness of the composite plies is 0.42 mm.

The mathematical representation of Problem 2 is defined as

Minimize: $F_{T[1]}$ (Tsai-Wu Failure Index at first layer)

Constraints: $\{F_{\text{Tsai-Wu}}, F_{\text{Hashin-Rotem}}, F_{\text{Maximum Stress}}\} \leq 1, \sigma_{\text{von-Misses}} < \sigma_{\text{yield}}$,

$-90^0 \leq \{\theta_1, \theta_2, \theta_3, \dots\} \leq 90^0, \{\theta_1, \theta_2, \theta_3, \dots\} \in \text{Integers}$,

$P_{\text{burst}} > 157.5 \text{ MPa}$,

Symmetric & Balance stacking sequences:

$[\pm\theta_1/\pm\theta_2/\pm\theta_3/ \dots/\mp\theta_3/\mp\theta_2/\mp\theta_1]$,

$t_{\text{ply}} = 0.42 \text{ mm}, t_{\text{liner}} = 1.8 \text{ mm}$

Problem 3

The main objective of the optimization problem 1 is to see significance of reduction in thickness of the ply, even though the total thickness of the composite part remains unchanged. For this reason, there are two different thicknesses to be 0.42 mm and 0.21 mm. DE have been used for two different design cases.

Minimize: $F_{T[1]}$ (Tsai-Wu Failure Index at first layer)

Constraints: $F_{\text{Tsai-Wu}} \leq 1$,

$-90^0 \leq \{\theta_1, \theta_2, \theta_3, \dots\} \leq 90^0$,

$P_{\text{burst}} > 110 \text{ MPa}$,

Stacking Sequences; $[\theta_1/\theta_2/\theta_3/ \dots]$,

$t_{\text{liner}} = 1.8 \text{ mm}$

7.2 Design Results of the problem 1, 2 and 3

After the solution of the optimization problem 1, two different stacking sequences designs of composites having burst strength over the 170 Mpa have been proposed (See Table 7.4). As DE have reached solution at 24 layers, SA managed to solve at 28 layers. There are two design results satisfying 70 Mpa working pressure and 2.25 safety factor in Problem 2. DE and SA results have also been compared with each other in the view of finding global optimum. As an optimum stacking sequences, DE have proposed design of fiber orientation configuration at 20 layers, whereas SA have suggested a 24 layered solution. It should be noted that, designs 1 and 2 proposed based on DE and SA have symmetric, balanced and integer fiber orientation angles, therefore, it provides easy manufacturable structures. According to results of composite design problems 1 and 2, DE is more effective than SA and.

In design problem 3, two design results with 10 and 20 layers capable of the strength over 110 Mpa have been proposed by using DE. The first design in problem 3 has 20 layers with 0.21 mm and 112 MPa burst pressure. The second has also 10 layers with 0.42 mm and 110 MPa. Even though the total thickness is not changed, difference of burst pressure between 10 and 20 layers the design is %0.018 in terms of the burst pressure.

In these problems, optimal design of cylindrical part of Type III tanks subjected to three different internal pressures have been performed by using DE and SA methods. Optimal design algorithms have composed of stress analysis, failure analysis and DE and SA methods.

Table 7.4 : Results of Problems.

Prob. No	Obj. Func.	Constraints	Optim. Alg.	Ply Thicknes (mm)	Stacking Sequences	Ply No	Burst Press. (MPa)
1	$F_{T(1)}$	$F_{Tsai-Wu} \leq 1$	DE	0.42	$[90_2/\mp 46/\pm 45/\mp 61/\pm 46/\pm 50]_s$	24	172
		$F_{Hashin-Rotem} \leq 1$, $F_{Maximum\ Stress} \leq 1$ $\theta \in \text{Integers}$ Symmetric-Balanced $P_{burst} > 170 \text{ MPa}$	SA	0.42	$[90_2/\mp 27/\pm 59/\mp 54/\pm 85/\mp 48/\mp 32]_s$	28	176
2	$F_{T(1)}$	$F_{Tsai-Wu} \leq 1$	DE	0.42	$[\mp 54/\pm 54/\pm 54/\mp 54/\pm 66]_s$	20	157.5
		$F_{Hashin-Rotem} \leq 1$, $F_{Maximum\ Stress} \leq 1$ $\theta \in \text{Integers}$ Symmetric-Balanced Safety Factor= 2.25 $P_{working}=70 \text{ MPa}$ $P_{burst}>157.5 \text{ MPa}$	SA	0.42	$[\pm 87/\pm 45/\pm 68/\mp 65/\mp 42/\pm 29]_s$	24	157.5
3	$F_{T(1)}$	$F_{Tsai-Wu} \leq 1$		0.42	$[85.2/47.5/53/47.5_2/-53_3/47.5/-53]$	10	110
		$\theta \in \{-90,90\}$ $P_{burst}>110 \text{ MPa}$	DE	0.21	$[90/-52_2/51.9_2/-52/51.9_2/-52_2/51.9_2/-52_2/51.9_3/-52_3]$	20	112

Two optimization method DE and SA have been compared. Different designs for hydrogen storage tanks have been reached. Due to be symmetric balanced and integer features of the composites, manufacturable stacking sequences design have been achieved. Finally, the results of the present study problems 1-3 can be concluded as:

- For problem 3, despite of the same total thickness, doubling of the number of layers haven't made an advantage in terms of burst pressure.
- By using DE and SA, two designs; $[90_2/\mp 46/\pm 45/\mp 61/\pm 46/\pm 50]_s$ and $[90_2/\mp 27/\pm 59/\mp 54/\pm 85/\mp 48/\mp 32]_s$ with 24 and 28 layers have been suggested as manufacturable designs. Both designs are capable of the burst strength over the 170 MPa.
- Two different stacking sequences; $[\mp 54/\pm 54/\pm 54/\mp 54/\pm 66]_s$ and $[\pm 87/\pm 45/\pm 68/\mp 65/\mp 42/\pm 29]_s$ composed of 20 and 24 layers have been carried at 157.5 Mpa burst pressure.

- According to comparison of the optimization results, the computational performance of DE is better than of SA to find global optimum of design problems for composite pressure vessel.

7.3 Problem 4

The main aim of the Problem 4 is to see effect of usage different Carbon/Epoxy materials on the design and optimization of the Type III hydrogen storage tanks. The materials considered in this problem and their properties are listed in Table 7.5. Thickness of the each lamina (t_{liner}) and radius of the tanks (R) are 1.8 and 200 mm, respectively. In the failure index calculations the strength properties of the materials are taken from references [62],[63] and [24].

The mathematical representation of Problem 4 is defined as

Minimize: $F_{T[1]}$ (Tsai-Wu Failure Index at first layer)

Constraints: $\{F_{\text{Tsai-Wu}}, F_{\text{Hashin-Rotem}}, F_{\text{Maximum Stress}}\} \leq 1,$

$\{\theta_1, \theta_2, \theta_3, \dots\} \in \{0, 15, 30, 45, 60, 75, 90\}$

$P_{\text{burst}} > 35$ MPa, Symmetric & Balance stacking sequences:

$[\pm\theta_1/\pm\theta_2/\pm\theta_3/ \dots/\mp\theta_3/\mp\theta_2/\mp\theta_1]$

Table 7.5 : Mechanical Properties of the materials.

	E_1 (GPa)	E_2 (GPa)	G_{12} (GPa)	ν_{12}	σ_{yield} (MPa)
T6061Al [62]	70	70	26.92	0.3	246
Carbon/Epoxy (T700)[62]	181	10.3	5.17	0.28	-
Carbon/Epoxy (IM6/SC1081)[63]	177	10.8	7.6	0.27	-
Carbon/Epoxy (T700s)[24]	135	9.66	5.86	0.25	

The optimization problem given above have been solved for different three Carbon/Epoxy materials. After the solution of the optimization problems, three different stacking sequences design of Type III pressure vessel having burst pressure over the 35 MPa have been reached. According the results:

- (i) it is seen that obtaining distinct designs having total thickness satisfying over 35 MPa burst pressure are possible.
- (ii) All of the designs have symmetric, balanced and integer fiber orientation angles, therefore, it provides easy manufacturable productions.

Table 7.6 : Optimization results of the Problem 4 for different Carbon/ Epoxy composites

Design Cases	Material	Ply Thickness (mm)	Stacking Sequences	Ply No	Total Thickness (mm)
a	Carbon/Epoxy (T700)	0.42	$[90_2/\mp 60/\pm 45/\mp 45/\mp 45/\pm 45]_s$	28	11,76
b	Carbon/Epoxy (T700)	0.127	$[90_2/\mp 30/90_2/\pm 60/\pm 30/90_4/\pm 45/\pm 45/\pm 60/\mp 30/\pm 30/90_4/\pm 45/\pm 30/90_4/\mp 45/\mp 45]_s$	80	10,16
c	Carbon/Epoxy (IM6/S C1081)	0.127	$[90_2/\pm 30/\mp 75/\pm 60/\pm 60/\pm 30/\pm 45/90_4/\pm 30/\pm 60/\pm 45/\mp 45/\pm 30/90_2/\pm 30/\mp 45/\mp 30/90_2/\pm 45/\mp 45/\pm 30/90_4/\mp 75/\mp 45/90_2]_s$	112	14,224

It can be said that, because of different mechanical properties, designs significantly vary in terms of stacking sequences even for the same type of materials. Additionally, small variations on thickness of the ply found to having big importance for the same material types.

7.4 Problem 5

In Problem 5, the primary objective is to see effects of the different Carbon/Epoxy materials on optimum stacking sequences design of Type V composite pressure vessel. In the beginning, the distributions of stress components based on CLPT have been calculated for composite pressure vessels. Then, the burst pressure of the composite pressure vessel is determined by using Tsai-Wu failure criterion and compared with analytical and experimental ones from literature. In the final step of the problem, for different Carbon/Epoxy materials that selected from the literature, the best possible combination of winding, stacking sequences and total thicknesses of laminates that satisfied 35 MPa for Tsai-Wu first ply failure criterion have been obtained by using DE stochastic optimization methods. All of the designs have symmetric, balanced and integer fibre orientation angles, therefore, they satisfy the manufacturing constraints.

The mathematical representation of Problem 5 is defined as

Minimize: $F_{T[1]}$ (Tsai-Wu Failure Index at first layer)

Constraints: $\{F_{\text{Tsai-Wu}}\} \leq 1,$

$\{\theta_1, \theta_2, \theta_3, \dots\} \in \{0, 15, 30, 45, 60, 75, 90\}$

$P_{\text{burst}} > 35 \text{ MPa},$

Symmetric & Balance stacking sequences:

$[\pm\theta_1/\pm\theta_2/\pm\theta_3/ \dots/\mp\theta_3/\mp\theta_2/\mp\theta_1]$

$R = 200 \text{ mm}$

Table 7.7 : Results of the Problem 5

Design Cases	Material	Ply Thickness (mm)	Stacking Sequences	Ply No	Total Thickness (mm)
a	Carbon/Epoxy (T700s)	0.42	$[\pm 75/\mp 45/\pm 45/\mp 45/\pm 45/\mp 75]_s$	24	10.08
b	Carbon/Epoxy (T700)	0.127	$[0_2/\pm 60/\mp 60/\mp 45/\pm 45/\mp 60/\pm 60/\pm 60/\pm 60]_s$	36	10,16
c	Carbon/Epoxy (IM6/SC1081)	0.127	$[\pm 90/\mp 75/\pm 30/\mp 90/0_2/\mp 90_2/\pm 75/\pm 90/\mp 15/\pm 45/\mp 90/\pm 75/\mp 90/\pm 90/\pm 75/\pm 90/\mp 60/0_4/\mp 60/\pm 15/\mp 90/\mp 15/\pm 75/\mp 75]_s$	104	14,224

Even for the three Carbon/Epoxy materials in close proximity to each other, design and optimization results have crucially changed. Besides of this, small differences in thicknesses of the laminates have shown dramatic variations on the stacking sequences designs.

7.5 Problem 6

In this problem, an optimization of the stacking sequences design has been investigated for Type III composite pressure vessel including aluminum liner. There are two important aim of the study: (i) to propose safety designs of symmetric-balanced stacking sequences over 140 Mpa and (ii) to compare the computational performance of Nelder Mead, Simulated Annealing and Differential Evolution methods on the solution of optimum design problems for Type III composite pressure vessel. Additionally, Tsai-Wu failure index of all the layers have been proposed to be less than 1. The maximum Tsai Wu failure index of all the layers are taken as objective function. Tsai Wu failure indexes and integers fiber orientation angles have been given as constraints. In the calculations, thicknesses of the composite layers and aluminum liner are taken as 0.127 mm and 3 mm, respectively. The radius of the tank is 100 mm. The material (Carbon/ Epoxy composite and aluminum) properties used in Problem 6 are given in Tables 6.8 and 6.9.

The mathematical representation of Problem 6 is

Minimize: $F_{T[1]}$ (Tsai-Wu Failure Index at first layer)

Constraints: $\{F_{\text{Tsai-Wu}}\} \leq 1,$

$-90^0 \leq \{\theta_1, \theta_2, \theta_3, \dots\} \leq 90^0, \{\theta_1, \theta_2, \theta_3, \dots\} \in \text{Integers}$

$P_{\text{burst}} > 140$ MPa, Symmetric & Balance stacking sequences,

Symmetric & Balance stacking sequences:

$[\pm\theta_1/\pm\theta_2/\pm\theta_3/ \dots/\mp\theta_3/\mp\theta_2/\mp\theta_1]$

$t_{\text{liner}} = 3$ mm, $R = 100$ mm, $t_{\text{ply}} = 0.127$ mm

Table 7.8 : Mechanical properties of T6061 Al and T700 Carbon/Epoxy composite materials [24]

	$E_1(\text{GPa})$	$E_2(\text{GPa})$	$G_{12}(\text{GPa})$	ν_{12}	ν_{23}	$\sigma_{\text{ult}} (\text{MPa})$
T6061Al	70	70	26.92	0.3	0.3	310
T700 Carbon/Epoxy	181	10.3	5.86	0.28	0.49	-

Table 7.9 : Strength parameters of T700 Carbon/Epoxy composite materials [24]

$\sigma_{1\text{ult}}^T (\text{MPa})$	$\sigma_{1\text{ult}}^C (\text{MPa})$	$\sigma_{2\text{ult}}^T (\text{MPa})$	$\sigma_{2\text{ult}}^C (\text{MPa})$	$\tau_{12\text{ult}} (\text{MPa})$
2150	-2150	298	-298	778

Table 7.10 : Optimum results of the stacking sequences design for problem 6

Optim. Alg.	Max. Tsai Wu Index	Stacking Sequences	Number of Plies	Total Thickness
DE	0.86	[90 ₃₆]	36	7.572
NM	0.89	[±89/∓85/∓85/∓87 ₂ /∓88/∓85/±89/∓86] _s	36	7.572
SA	0.98	[∓70/90 ₂ /∓82/90 ₆ /∓74/90 ₂ /±76] _s	36	7.572

As a result of the problem 6, three different stacking sequences designs of the cylindrical part of the Type III pressure vessel satisfying burst strength over the 140 MPa have been obtained (see Table 6.10). Maximum failure index of all plies for each problem have been minimized by DE, SA and NM. According to comparison of the results based on these methods, DE, NM and SA have reached the global minimums as 0.86, 0.89 and 0.98 for the 36 plies, respectively. It is seen that the computational performance of DE on finding optimum failure index is better than those of NM and SA and NM are better than SA. Unlike the other problems in this thesis, the objective functions have been selected as maximum Tsai Wu failure index of all plies. Additionally, in Problem 6, the number of layers and fiber orientation angles are optimized simultaneously.



8. CONCLUSION

In this thesis, the failure analysis and the optimum designs of composite hydrogen storage tanks have been investigated. The optimizations have been carried out by different Aluminium-Carbon/Epoxy (Type III), Graphite/Epoxy and Carbon/Epoxy (Type V) materials. The number of plies and fiber orientation angles of the laminated composites are taken as design variables. Single-objective optimization approach has been selected for design and mathematical verification of model problems. Non-traditional search techniques: Differential Evolution (DE), Simulated Annealing (SA) and Nelder Mead (NM) have been considered as optimization methods. MATHEMATICA commercial software has been used in the stress and failure analysis and optimization process. Optimal designs of Type III and Type V hydrogen storage tanks subjected to different internal pressures have been proposed. In order to see the computational performance of considered optimization algorithms, the same design problems have been solved separately by DE, SA and NM. Different stacking sequences designs for hydrogen storage tanks have been introduced for the same burst pressure limit. Classical Laminated Plate Theory and the first ply failure theories including Tsai-Wu, Hashin-Rotem and Maximum Stress have been utilized to calculate burst pressure for different composite pressure vessels (Type III, Type IV and Type V). The burst pressure calculations for Type III and Type V hydrogen storage tanks have been compared with the experimental and Finite Element Method results from literature. After the validation of the burst pressure predictions, optimization algorithms have been run to solve different design problems selected from the literature. Additionally comparison of the DE, SA and NM algorithms each other have been carried out on Type III composite pressure vessel problems.

- In the Problems V1, V2 and V3 burst pressure predictions have been validated for Type V pressure vessels, computational performance of the DE, SA and NM have been compared with Genetic Algorithms (GA). It is seen that DE,

SA and NM show better performance than GA in some cases. Parametric calculations have been achieved for first ply failure indexes, burst pressure, areal mass density and hoop rigidity of the composite pressure vessel.

- In the Problem V1, the comparison of the results for burst pressure, areal mass density and hoop rigidity from the literature [Pelletier and Vel, 2006], shows that results are reached same value.
- By using DE and SA, two designs with 24 and 28 layers have been suggested as manufacturable designs. Both designs are capable of the burst strength over the 170 Mpa.
- For Type III and Type V hydrogen storage tanks, the burst pressure calculations have been compared with the experimental and Finite Element Method results from literature. It is shown that there are good agreement among the results.
- Different stacking sequences of fiber orientation angles composed of 20 and 24 layers have been proposed against to 157.5 Mpa burst pressure.
- For Problem 3, despite of the same total thickness, doubling of the number of layers haven't made an advantage in terms of burst pressure.
- Burst pressure predictions based on Tsai-Wu first ply failure criterion for Type V pressure vessels are very close to results compared to experimental results. It can be seen that the maximum errors for three cases have varied between the 15% and 2%. Therefore, the prediction capability of the present steps is appropriate.
- The optimization problems of the Type III and Type V hydrogen storage tanks have been solved by DE, NM and SA. The results have been compared to each other and it is found that the computational performance of DE on finding optimum failure index is better than those of NM and SA and NM are better than SA. The optimization algorithms DE, SA and NM have given the applicable results for composite hydrogen storage tanks designs problems. Due to be symmetric balanced and integer features of the composites, manufacturable stacking sequences design have been achieved.
- In the Problem 6, unlike the other problems in this thesis, the objective functions have been selected as maximum Tsai Wu failure index of all plies as a new approach.

- Even for the three Carbon/Epoxy materials in close proximity to each other, design and optimization results have crucially changed. It can be concluded that the generalization for optimum stacking sequences of Carbon/ Epoxy materials should be avoided.





REFERENCES

- [1]. Cohen, D. (1997). Influence of filament winding parameters on composite vessel quality and strength. *Composites Part A*, 28(A), 1035-1047.
- [2]. Chapelle, D. Perreux, D. (2006). Optimal design of a type 3 hydrogen vessel: Part IeAnalytic modelling of the cylindrical section. *Int J Hydrogen Energy*, 31(5), 627e38.
- [3]. Hu, J., Chen, J., Sundararaman, S., Chandrashekhara, K., Chernicoff, W., (2008). Analysis of composite hydrogen storage cylinders subjected to localized flame impingements. *Int J Hydrogen Energy*, 33(11), 2738e46.
- [4]. Onder, A. Sayman, O. Dogan, T. Tarakcioglu, N. (2009). Burst failure load of composite pressure vessels. *Compos Struct*, 89(1), 159e66.
- [5]. Xu, P. Zheng, J. Liu, P. (2009). Finite element analysis of burst pressure of composite hydrogen storage vessels. *Mater Des*, 30(7), 2295e301.
- [6]. Hu, J. Chandrashekhara, K. (2009). Fracture analysis of hydrogen storage composite cylinders with liner crack accounting for autofrettage effect. *Int J Hydrogen Energy*, 34(8), 3425e35.
- [7]. Camara, S. Bunsell, AR. Thionnet, A. Allen, DH. (2011) Determination of lifetime probabilities of carbon fibre composite plates and pressure vessels for hydrogen storage. *Int J Hydrogen Energy*, 2011, 36(10), 6031e8.
- [8]. Son, DS. Chang, SH. (2012). Evaluation of modeling techniques for a Type III hydrogen pressure vessel (70 MPa) made of an aluminum liner and a thick Carbon/Epoxy composite for fuel cell vehicles. *Int J Hydrogen Energy*, 37(3), 2353e69.
- [9]. Liu, P. Chu, J. Hou, S. Zheng, J. (2012). Micromechanical damage modeling and multiscale progressive failure analysis of composite pressure vessel. *Comput Mater Sci*, 60, 137e48.

- [10]. Leh, D. Saffre, P. Francescato, P. Arrieux, R. (2013). Multi-sequence dome lay-up simulations for hydrogen hyper-bar composite pressure vessels. *Compos Part A Appl Sci Manuf*, 52, 106e17.
- [11]. Liu, PF. Chu, JK. Hou, SJ. Xu, P. Zheng, JY. (2012). Numerical simulation and optimal design for composite high-pressure hydrogen storage vessel: a review. *Renew Sustain Energy Rev*, 16(4), 1817e27.
- [12]. Messenger, T. Pyrz, M. Gineste, B. Chauchot, P. (2002). Optimal Laminations of Thin Underwater Composite Cylindrical Vessels. *Composite Structure*, 58:529–37.
- [13]. Parnas, L. Katirci, N. (2002). Design of Fiber-Reinforced Composite Pressure Vessels Under Various Loading Conditions, *Composite Structure*, 58:83–95.
- [14]. Tabakov, P.Y. (2001). Multi-Dimensional Design Optimization of Laminated Structures Using an Improved Genetic Algorithm. *Composite Structure*, 54:349–54.
- [15]. Richard, F. Perreux, D. (2000). A reliability method for optimization of [+h/_h]_n fiber reinforced composite pipes, *Reliab Eng Syst Saf*, 68:53–9.
- [16]. Kim, C.U. Hong, C.S. Kim, C.G Kim, J.Y. (2005). Optimal Design Of Filament Wound Type 3 Tanks Under Internal Pressure Using a Modified Genetic Algorithm. *Composite Structure*, 71(1), 16e25.
- [17]. Tomassetti, G. Barboni, R. Benedetti, M. (2005). Optimisation Methodology for Cryotanks”, *Computational Structure*, 83(28), 2293e305,.
- [18]. Liu, P. Xu, P. Zheng, J. (2009). Artificial Immune System for Optimal Design of Composite Hydrogen Storage Vessel. *Computational Materials Science*, 47(1), 261e7.
- [19]. Xu, P. Zheng, J. Chen, H. Liu, P. (2010). Optimal Design of High Pressure Hydrogen Storage Vessel Using an Adaptive Genetic Algorithm, *International Journal of Hydrogen Energy*, 35(7), 2840e6.
- [20]. Francescato, P. Gillet, A. Leh, D. Saffré, P. (2012). Comparison of Optimal Design Methods for Type 3 High-Pressure Storage Tanks. *Composite Structures*, 94, 2087–2096.
- [21]. Roh, H. Hua, T. Ahluwalia, R. (2013). Optimization of Carbon Fiber Usage In Type 4 Hydrogen Storage Tanks for Fuel Cell Automobiles. *International Journal of Hydrogen Energy*, 38(29),12795e802.

- [22]. Alcantar, V. Aceves, S.M. Ledesma, E. Ledesma, S. Aguilera, E. (2017). Optimization of Type 4 Composite Pressure Vessels Using Genetic Algorithms and Simulated Annealing. *International Journal of Hydrogen Energy*, 0360-3199.
- [23]. Vafaeseefat A. (2011). Optimization of composite pressure vessels with metal liner by adaptive response surface method. *J Mech Sci Technol*, 25(11), 2811e6.
- [24]. Alcantar, V. Ledesma, S. Aceves, S.M. Ledesma, E. Saldana, A. (2017). Optimization of Type III Pressure Vessels Using Genetic Algorithms and Simulated Annealing. *International Journal of Hydrogen Energy*, 0360-3199.
- [25]. Aydın, L. Artem, H. S. (2017). Design and optimization of fiber composites. *Fiber Technology for Fiber Reinforced Composite*, Chapter 14, 299-312, ISBN: 978-0-08-101871-2, Woodhead Publishing Press.
- [26]. Ayakdaş, O. Aydın, L. (2017). Hydrogen storage technologies. *Researches on Science and Art in 21st Century Turkey*, Chapter 321, 2890-2899, ISBN: 978-605-288-062-3, Gece Kitapevi.
- [27]. Millet, P. (2014). Hydrogen storage in hydride-forming materials. *Advances in Hydrogen Production, Storage and Distribution*, Chapter 14, 368-406, ISBN 978-0-85709-768-2.
- [28]. Cerri, I. Lefebvre-Joud, F. Holtappels, P. Honegger, K. Stubos T. Millet, P. (2012). In: ‘Hydrogen and Fuel Cells’, Scientific Assessment in support of the Materials Roadmap enabling Low Carbon Energy Technologies”, JRC Scientific and Technical Reports.
- [29]. Bowman, B. Klebanoff, L. (2014). Historical Perspectives on Hydrogen, Its Storage, and Its Applications. *Hydrogen Storage Technology Materials and Applications*. Chapter 3. 65 - 85, ISBN 13: 978-1-4398-4108-2.
- [30]. Eberle, U. Felderhoff, M. Schüth, F.(2009). Chemical and Physical Solutions for Hydrogen Storage. *Angewandte Chemie International Edition*, 48:6608 – 6630.
- [31]. Helmolt, R. V. Eberle, U. (2007). Fuel Cell Vehicles: Status 2007. *J. Power Sources*, 165, 833–843.
- [32]. Barthélémy, H. (2012). Hydrogen Storage - Industrial Prospectives. *International Journal of Hydrogen Energy*, 37:17364-17372.

- [33]. Barthélémy, H. (2009). Hydrogen storage technologies: compatibility of materials with hydrogen. In Proceedings of the International Conference on Hydrogen Safety, Ajaccio, Corsica.
- [34]. Hua, T.Q. Ahluwalia, R.K. Peng, J.-K. Kromer, M. Lasher, S. McKenney, K. Law, K. Sinha., J. (2011). Technical Assessment of Compressed Hydrogen Storage Tank Systems for Automotive Applications, *International Journal of Hydrogen Energy*, 36:3037–3049.
- [35]. US DOE. (2009) US DOE Office of Energy Efficiency and Renewable Energy and the Freedom CAR and Fuel Partnership, Targets for Onboard Hydrogen Storage Systems for Light-Duty Vehicles.
- [36]. Toyota, (last access: 09. 08. 2017). Fcv fuel cell vehicle. http://www.toyotaglobal.com/innovation/environmental_technology/fuel_cell_vehicle/.
- [37]. Vogler & Würsig Eberle, U. Felderhoff, M. Schüth, F. (2009) Chemical and Physical Solutions for Hydrogen Storage. *Angewandte Chemie International Edition*, 48:6608 – 6630.
- [38]. Chacón, E. Martínez, G. Anchuelo, C. Cuevas, R. (2010). Unmanned Aerial Vehicle Driven by Fuel Cell Technology, AVIZOR. 18th World Hydrogen Energy Conference - WHEC 2010, 16-21 May 2010, Essen, 1866-1793.
- [39]. Berenberg, B. (2003). Towpreg Proves Cost-Competitive for Wound Pressure Vessels. *High Performance Composites, Design and Manufacturing, Solutions for Industry*, Ray Publishing, p.36.
- [40]. Mallick, P.K. (2008). Manufacturing. Fiber Reinforced Composites Materials, *Manufacturing And Design*, CRC Press, Chapter 5, 13: 978-0-8493-4205-9.
- [41]. CORDIS, (2006). “Tow-preg filament winding production process”, ZEM Report Summary - European Commission, 2006.
- [42]. Filament winding. Filment winding procces, [http:// www.nuplex.com/composites/processes/filament-winding](http://www.nuplex.com/composites/processes/filament-winding) (last access: 09.08.2017).
- [43]. Kaw, A. K. (2006). Mechanics of composite materials 2nd. *Optics Express* (Vol.18). Retrieved from <http://www.ncbi.nlm.nih.gov/pubmed/20725652>
- [44]. Vinson, J. R., Sierakowski, R. L. (2004). *The Behavior of Structures Composed of Composite Materials*. Kluwer Academic Publishers.

- [45]. Daniel, I. M., Ishai, O. (2005). Engineering Mechanics of Composite Materials. <https://doi.org/10.1016/B978-0-08-006421-5.50049-6>
- [46]. Pelletier, J. L., Vel, S. S., (2006). Multi-objective optimization of fiber reinforced composite laminates for strength, stiffness and minimal mass. *Computers and Structures*, 84, 2065-2080, doi:10.1016/j.compstruc.2006.06.001
- [47]. Hyer, M. W., White, S. R. (1998). Stress analysis of fiber-reinforced composite materials. WCB McGraw-Hill, ISBN: 0070167001.
- [48]. Aydin, L. Artem, H. S. Oterkus, E. Gundogdu, O. Akbulut, H. (2017) Mechanics of fiber composites, Fiber Technology for Fiber Reinforced Composite, Woodhead Publishing Press, Chapter 2, 5-48, ISBN: 978-0-08-101871-2.
- [49]. Hashin, Z. Rotem, A. (1973). A Fatigue Failure Criterion for Fibre Reinforced Materials. *J. Composite Materials*, v.7, 448-464.
- [50]. Aydin, L., & Artem, H. S. (2011). Comparison of stochastic search optimization algorithms for the laminated composites under mechanical and hygrothermal loadings. *Journal of Reinforced Plastics and Composites*, 30(14), 1197–1212.
- [51]. Gurdal, Z., Haftka, R. T., & Hajela, P. (1999). Design and optimization of laminated composite materials. John Wiley & Sons.
- [52]. Rao, S. S. (2009). *Engineering Optimization: Theory and Practice*. Wiley. <https://doi.org/10.1002/9780470549124>
- [53]. Storn, R., Price, K. (1997). Differential Evolution – A Simple and Efficient Heuristic for global Optimization over Continuous Spaces. *Journal of Global Optimization*, 11(4), 341–359. <https://doi.org/10.1023/A:1008202821328>
- [54]. Sivanandam, S. N., Deepa, S. N. (2008). *Introduction to Genetic Algorithms*. *Introduction to Genetic Algorithms*. Berlin, Heidelberg: Springer Berlin Heidelberg. <https://doi.org/10.1007/978-3-540-73190-0>
- [55]. Roque, C. M. C., & Martins, P. A. L. S. (2015). Differential evolution optimization for the analysis of composite plates with radial basis collocation meshless method. *Composite Structures*, 124, 317–326.
- [56]. Nelder, J. A., & Mead, R. (1965). A simplex-method for function minimization. *Computer Journal*, 7(4), 308–313. <https://doi.org/10.1093/comjnl/7.4.308>

- [57]. Fan, S.-K. S., Liang, Y.-C., & Zahara, E. (2006). A Genetic Algorithm and a Particle Swarm Optimizer Hybridized with Nelder-Mead Simplex Search.pdf. *Computers and Industrial Engineering*, 401–425.
- [58]. Vo-Duy, T., Ho-Huu, V., Do-Thi, T. D., Dang-Trung, H., & Nguyen-Thoi, T. (2017). A global numerical approach for lightweight design optimization of laminated composite plates subjected to frequency constraints. *Composite Structures*, 159, 646–655. <https://doi.org/10.1016/j.compstruct.2016.09.059>
- [59]. Barati, R. (2011). Parameter Estimation of Nonlinear Muskingum Models Using Nelder-Mead Simplex Algorithm. *Journal of Hydrologic Engineering*, 19(NOVEMBER), 1–8. [https://doi.org/10.1061/\(ASCE\)HE](https://doi.org/10.1061/(ASCE)HE)
- [60]. Pham, D., & Karaboga, D. (2000). *Intelligent optimisation techniques, genetic algorithms, tabu search, simulated annealing and neural network*. Springer, New York. <https://doi.org/10.1007/978-1-4471-0721-7>
- [61]. Chang R.R., (2000). Experimental and theoretical analyses of first-ply failure of laminated composite pressure vessel., *Composite Structures*, 49/ 237-243.
- [62]. Liu P.F., Xing L. J., Zheng J.Y., (2014). Failure analysis of carbon fiber/Epoxy composite cylindrical laminates using explicit finite element method, *Composite Part B*, 56/ 54-61.
- [63]. Mian H. H., Wang G., Dar U. A., Zhang W.,(2013). Optimization of Composite Material System and Lay-up to Achieve Minimum Weight Pressure Vessel, *Applied Composite Materials*. Volume 20, Issue 5, pp 873–889.
- [64]. Vasiliev V. V., Morozov E. V., (2007). *Advanced Mechanics of Composite Materials*. ISBN: 978-0-08-045372-9, Elsevier.

VITA

OZAN AYAKDAŞ

26-04-1991, AYDIN /TURKEY

EDUCATION

M.Sc. (2015-2018) : Mechanical Engineering, İzmir Katip Çelebi University

B.Sc (2009-2014) : Mechanical Engineering, Dokuz Eylül University

P.S. (2009-2010) : Preparation School (English), Dokuz Eylül University

INTERNATIONAL BOOK CHAPTER PAPERS

- **O. Ayakdaş**, L. Aydın, “Hydrogen Storage Technologies”, Researches on Science and Art in 21st Century Turkey, Book Chapter, 2017
- M. Savran, **O. Ayakdaş**, L. Aydın, “Free Vibration Analysis of Laminated Composite Plates”, The Most Recent Studies in Science and Art, Book Chapter, 2018
- S. Öztürk, E. Kayabası, N. Küçükdoğan, **O. Ayakdaş**, “Progress in Application of Black Silicon”, The Most Recent Studies in Science and Art, Book Chapter, 2018

INTERNATIONAL CONFERENCE PROCEEDINGS

- **O. Ayakdaş**, L. Aydın, H. S. Artem, H. Sayı, “Failure Analysis And Optimization Of The Cylindrical Part Of Type-III Hydrogen Storage Tanks”, 5th International Polymeric Composites Symposium and Workshops, 02-04 November 2017.
- H. Sayı, H. S. Artem, L. Aydın, **O. Ayakdaş**, “Stacking Sequences Design of Composite Hydrogen Storage Tanks Using Optimization Algorithms”, 5th International Polymeric Composites Symposium and Workshops, 02-04 November 2017.
- **Ozan Ayakdaş**, Levent Aydın , Melih Savran, Nilay Küçükdoğan, Savaş Öztürk, ” Design and Optimization of the Type III Pressure Vessel for Different Carbon/Epoxy Materials by using Differential Evolution Methods” , 1st International Symposium on Light Alloys and Composite Materials (ISLAC'18), March 22-24, 2018.

- Melih Savran, Levent Aydın, **Ozan Ayakdaş**, Savaş Öztürk, Nilay Öztürk, “Optimum Design of Glass/Epoxy and Flax/Epoxy Laminated Composite Plates for Maximum Frequency Using a Stochastic Optimization Method”, 1st International Symposium on Light Alloys and Composite Materials (ISLAC’18), March 22-24, 2018.
- Mehmet Akçair, Melih Savran, Levent Aydın, **Ozan Ayakdaş**, Savaş Öztürk, Nilay Küçükdoğan, “Optimum Design of Anti-Buckling Behaviour of Graphite/Epoxy Laminated Composite Plate Using Differential Evolution Method”, 1st International Symposium on Light Alloys and Composite Materials (ISLAC’18), March 22-24, 2018.

PROJECT

Design, Optimization and Prototype Production of High Pressure Durable Lightweight Composite Tank Materials and Systems for Hydrogen Storage and Distribution (TUBİTAK- 215M182 project 2016-2018)